


Cite this: *RSC Adv.*, 2020, 10, 34114

Synthesis, biological evaluation, and *in silico* studies of novel chalcone- and pyrazoline-based 1,3,5-triazines as potential anticancer agents†

Leydi M. Moreno,^a Jairo Quiroga,^{ab} Rodrigo Abonia,^{ab} Antonino Lauria,^c Annamaria Martorana,^c Henry Insuasty^d and Braulio Insuasty^{d*ab}

A novel series of triazin-chalcones (7,8)a–g and triazin-*N*-(3,5-dichlorophenyl)pyrazolines (9,10)a–g were synthesized and evaluated for their anticancer activity against nine different cancer strains. Triazine ketones 5 and 6 were synthesized from the cyanuric chloride 1 by using stepwise nucleophilic substitution of the chlorine atom. These ketones were subsequently subjected to a Claisen–Schmidt condensation reaction with aromatic aldehydes affording chalcones (7,8)a–g. Then, *N*-(3,5-dichlorophenyl)pyrazolines (9,10)a–g were obtained by cyclocondensation reactions of the respective chalcones (7,8)a–g with 3,5-dichlorophenylhydrazine. Among all the evaluated compounds, chalcones 7d,g and 8g exhibited more potent *in vitro* anticancer activity, with outstanding GI₅₀ values ranging from 0.422 to 14.9 μM and LC₅₀ values ranging from 5.08 μM to >100 μM. *In silico* studies, for both ligand- and structure-based, were executed to explore the inhibitory nature of chalcones and triazine derivatives. The results suggested that the evaluated compounds could act as modulators of the human thymidylate synthase enzyme.

Received 6th August 2020
Accepted 9th September 2020

DOI: 10.1039/d0ra06799g

rsc.li/rsc-advances

1. Introduction

Heterocycles constitute a structural scaffold in a wide range of drugs and have occupied a prominent place in medicinal chemistry due to their ability to imitate and interact with biological molecules thus exhibiting remarkable pharmacological properties.^{1–4} The utility of heterocyclic rings, such as triazines and pyrazolines in different areas of medicine, particularly as potential anticancer drugs continue to be investigated.^{5–8}

The 1,3,5-triazine is a versatile ring that can act as a scaffold to carry three functionalized branches at 2,4 and 6-positions and this property allows to easily modulate the physicochemical and biological properties of these derivatives.⁵ The anticancer activity mechanisms of these systems can be associated with different targets. Thus, 1,3,5-triazine-2-carbohydrazides exhibited Rad6B inhibitory activity,⁹ while macrocyclic pyrazolo[1,5-*a*] [1,3,5]triazines showed potent inhibition of CK2 protein kinase.¹⁰ Other mechanisms of action are related to the inhibition of phosphatidylinositol 3-kinase α /mammalian target of

rapamycin (PI3K α /mTOR),¹¹ carbonic anhydrase (CA),^{12–14} human topoisomerase II α ,¹⁵ dihydrofolate reductase (dHFR)¹⁶ and tubulin polymerization¹⁷ (Fig. 1).

Similarly, pyrazoline rings are quite promising fragments due their anticancer properties. Pyrazoline hybrids with heterocyclic rings such as imidazopyridine,⁸ thiazole,¹⁸ triazine,^{19,20} 4-thiazolidinone-indole²¹ and dihydroquinolone²² have been reported as potential anticancer agents. Pyrazoline rings can be easily obtained by a cyclocondensation reaction of chalcones with hydrazine derivatives.²³ Chalcones have also shown marked biological activity as anticancer agents,^{24–26} that allows comparative studies of antiproliferative activity to be carried out between the precursor chalcones and the pyrazolinic derivatives and at the same time expand the mosaic of compounds evaluated.

The enzyme thymidylate synthase (TS) is an E2F1-regulated enzyme that is essential for DNA synthesis and repair. TS and mRNA levels are elevated in many human cancers, and high TS levels have been correlated with poor prognosis in patients with colorectal, breast, cervical, bladder, kidney, and non-small cell lung cancers.²⁷ Inhibition of TS causing cells incapable of undergoing accurate DNA replication, ultimately leading to cell death.^{28,29} Owing to their important role in cell, TS represent a natural target for anticancer therapies.

In a preliminary work we reported the synthesis and anticancer activity of chalcone- and pyrazoline-based 1,3,5-triazines.²⁰ Several of these tested molecules showed low toxicity and outstanding antiproliferative activity against a wide range of cancer cell lines with GI₅₀ values in the range of 0.569–16.6

^aHeterocyclic Compounds Research Group, Department of Chemistry, Universidad del Valle, A.A. 25360 Cali, Colombia. E-mail: braulio.insuasty@correounivalle.edu.co

^bCenter for Bioinformatics and Photonics-CIBioFI, A.A. 25360 Cali, Colombia

^cDipartimento di Scienze e Tecnologie Biologiche Chimiche e Farmaceutiche “STEBICEF”, Università di Palermo, Viale delle Scienze Ed. 17, I-90128 Palermo, Italy

^dHeterocyclic Compounds Research Group, Department of Chemistry, Universidad de Nariño, A.A. 1175 Pasto, Colombia

† Electronic supplementary information (ESI) available: Table S1, spectra data and Fig. S1. See DOI: 10.1039/d0ra06799g



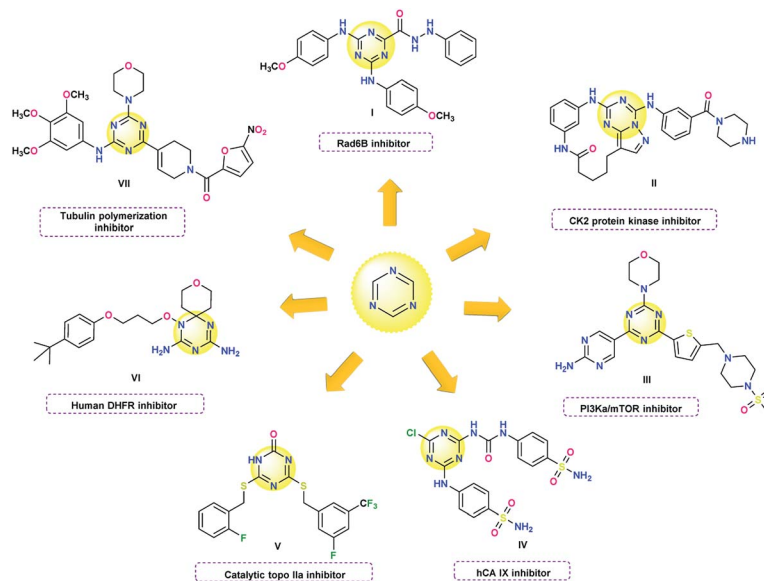


Fig. 1 Triazine derivatives with different anticancer activity mechanisms.

μM . A raw SAR analysis showed that *N*-(3,5-dichlorophenyl) pyrazolines and chalcones were the most active molecules. According to the previously described, we focused on the promising trisubstituted-1,3,5-triazinic systems and decided to synthesize and evaluate a new series of *N*-(3,5-dichlorophenyl) pyrazoline and chalcone based 1,3,5-triazines as anticancer agents. Additionally, *in silico* studies were done to help understand the possible mode of action of the new active compounds.

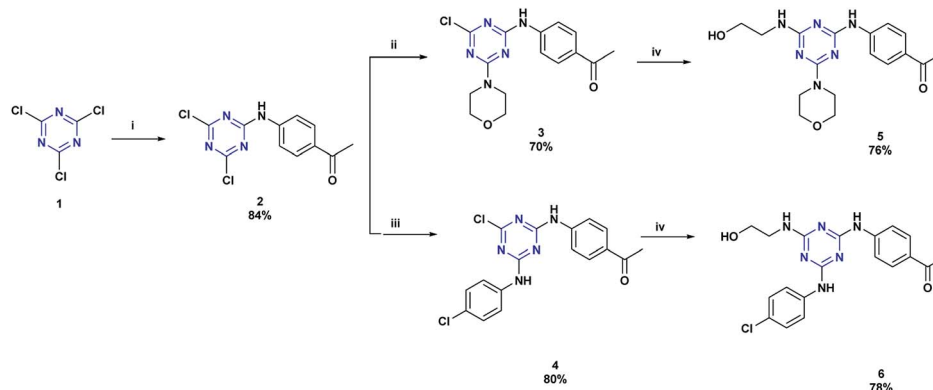
2. Results and discussion

2.1. Chemistry

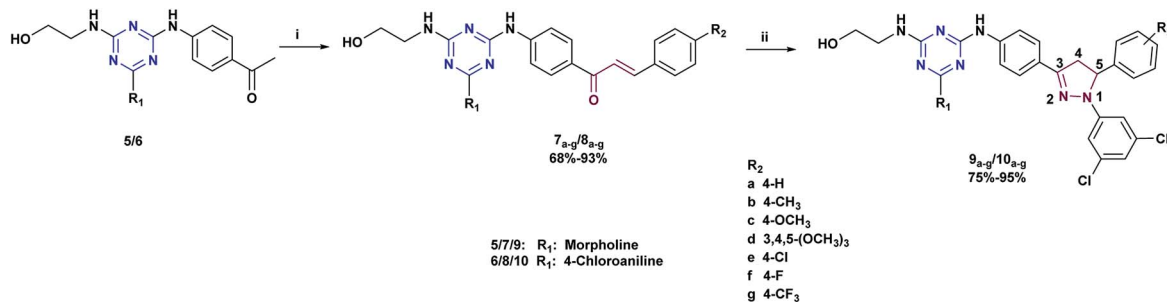
The target compound **9a–g** and **10a–g** were obtained by a multi-stage synthesis as described in Schemes 1 and 2. Initially, 2,4,6-trichloro-1,3,5-triazine **1** was submitted to consecutive nucleophilic substitution reactions: first with 4-aminoacetophenone, then with morpholine or 4-chloroaniline and finally with ethanolamine, under the conditions described in Scheme 1, to afford the respective 2,4,6-trisubstituted-1,3,5-triazines **5** and **6**

in excellent yields. These precursors were characterized by FTIR, $^1\text{H-NMR}$, $^{13}\text{C-NMR}$, and mass spectrometry (see Experimental section).

(*E*)-1-(4-((4-((2-hydroxyethyl)amino)-6-morpholino-1,3,5-triazin-2-yl)amino)phenyl)-3-(substituted)chalcones **7a–g** and (*E*)-1-(4-((4-((4-chlorophenyl)amino)-6-((2-hydroxyethyl)amino)-1,3,5-triazin-2-yl)amino)phenyl)-3-(substituted)chalcones **8a–g** were obtained from triazine-ketones **5** and **6**, respectively, by Claisen–Schmidt condensation reaction with substituted benzaldehydes in the presence of 20% KOH solution in EtOH (Scheme 2). The structures of chalcones **7a–g** and **8a–g** were confirmed by spectroscopic techniques (FTIR, $^1\text{H-NMR}$, $^{13}\text{C-NMR}$ and mass spectrometry). These compounds showed wide FTIR absorption bands in the range of $3277\text{--}3315\text{ cm}^{-1}$ assigned to O–H groups. The IR spectra also showed absorption bands at $1641\text{--}1651$, $1560\text{--}1587$ and $1506\text{--}1558\text{ cm}^{-1}$ assigned to C=O, C=N and C=C functionalities, respectively. In the $^1\text{H-NMR}$ spectrum of chalcone **7e**, for example, the signal of the vinylic proton H_β of the α,β -unsaturated system appears as



Scheme 1 Synthetic pathway for triazine derivatives **5** and **6**. Reagents and conditions: (i) 4-aminoacetophenone; acetone, $-5\text{--}0\text{ }^\circ\text{C}$, 5 h; (ii) morpholine, acetone, $-5\text{--}0\text{ }^\circ\text{C}$, 6 h; (iii) 4-chloroaniline, dioxane, room temperature, 12 h; (iv) ethanolamine, dioxane, reflux, 8 h.



Scheme 2 Synthesis of *N*-(3,5-dichlorophenyl)pyrazolines **9a–g** and **10a–g** and their precursor chalcones **7a–g** and **8a–g**. Reagents and conditions: (i) benzaldehyde- R_2 , 20% KOH, ethanol, 3–8 h; (ii) 3,5-dichlorophenylhydrazine hydrochloride, ethanol, reflux, 12 h.

a doublet at 7.68 ppm with a coupling constant of $^3J = 15.6$ Hz, which agrees with a *E*-configuration. The signal of other vinyl proton H_α appears overlapped with signals of aromatic protons at 7.89–7.99 ppm. In the ^{13}C -NMR spectrum the signals of α and β carbon atoms were observed at 118.4 and 141.4 ppm, respectively. The mass spectrum shows molecular ion peak at m/z 480 and with a isotopic profile of 12 : 4 ($[M]^+ : [M + 2]^+$), characteristic of a compound bearing one chlorine atom in its structure.

Reaction of the synthesized chalcones **7a–g** and **8a–g** with 3,5-dichlorophenylhydrazine hydrochloride in ethanol under reflux afforded *N*-(3,5-dichlorophenyl)pyrazolines **9a–g** and **10a–g** (Scheme 2), respectively, in racemic mixtures. Taking as example compound **9e**, in the ^1H -NMR spectrum, the formation of the pyrazoline ring is confirmed by the appearance of two double doublets at 3.15 ppm (with $^2J_{\text{AM}} = 17.7$ Hz and $^3J_{\text{AX}} = 4.4$ Hz), and at 3.92 ppm (with $^2J_{\text{AM}} = 17.7$ Hz, and $^3J_{\text{MX}} = 11.7$ Hz) corresponding to protons on the diastereotopic center C-4,

Table 1 Mean growth, %GI and lethality values for the most sensitive cell lines displayed by the tested compounds against 60 NCI human cancer cell lines at 10 μM

Compound	Mean growth	Most sensitive cell line	Growth inhibition percent (%GI) ^a /lethality ^b
5	97.18	SNB-75 (CNS cancer)	33.36
6	89.48	SR (leukemia)	35.27
7a	81.57	SR (leukemia)	87.24
7b	95.32	UACC-62 (melanoma)	27.15
7c	87.49	MCF7 (breast cancer)	70.68
7d	17.60	UACC-62 (melanoma)	−31.70 ^{b,c}
7e	77.12	MCF7 (breast cancer)	90.27
7f	79.95	MCF7 (breast cancer)	88.77
7g	34.86	U251 (CNS cancer)	−51.34 ^{b,c}
8a	71.26	HCT-15 (colon cancer)	91.45
8b	77.30	MCF7 (breast cancer)	78.50
8c	68.77	RPMI-8226 (leukemia)	91.94
8d	69.89	MOLT-4 (leukemia)	84.74
8e	58.28	HCT-116 (colon cancer)	−78.88 ^a
8f	67.99	RPMI-8226 (leukemia)	98.22
8g	42.92	HCT-116 (colon cancer)	−85.59 ^{b,c}
9a	82.34	UACC-62 (melanoma)	45.95
9b	93.57	MCF7 (breast cancer)	33.41
9c	87.26	MCF7 (breast cancer)	45.02
9d	50.41	RXF 393 (renal cancer)	94.92
9e	84.61	MCF7 (breast cancer)	43.41
9f	74.76	786-0 (renal cancer)	67.01
9g	72.39	RXF 393 (renal cancer)	80.30
10a	95.13	HS 578T (breast cancer)	29.35
10b	96.74	HS 578T (breast cancer)	31.73
10c	90.95	UO-31 (renal cancer)	35.19
10d	74.43	MOLT-4 (leukemia)	65.16
10e	95.42	HS 578T (breast cancer)	35.59
10f	94.58	HS 578T (breast cancer)	38.64
10g	99.72	HS 578T (breast cancer)	26.04

^a %GI (growth inhibition percentage) = 100 − GP (growth percentage). ^b Negative values mean lethality of the respective cancer cell line.

^c Compounds with the most relevant inhibitory activity against all cancer cell lines in terms of their mean values.



Table 2 Antiproliferative activity (GI_{50}^a and LC_{50}^b) displayed by compounds **7d,g** and **8g** against 60 human cancer cell lines^c compared with the standard drug 5-FU

		Compounds							
Panel name	Cell name	7d		7g		8g		5-FU NS 18893 ^d	
		GI ₅₀ ^a	LC ₅₀ ^b	GI ₅₀	LC ₅₀	GI ₅₀	LC ₅₀	GI ₅₀	LC ₅₀
Leukemia	CCRF-CEM	0.935	>100	2.41	>100	2.75	>100	10.00	>100
	HL-60(TB)	1.79	>100	2.92	>100	12.2	>100	2.51	>100
	K-562	0.783	>100	2.33	>100	2.83	>100	3.98	>100
	MOLT-4	1.19	>100	2.45	>100	3.56	>100	0.32	>100
	RPMI-8226	0.612	—	2.07	>100	1.56	>100	0.05	>100
Non-small cell lung cancer	SR	0.422	>100	3.1	>100	1.95	>100	0.03	>100
	A549/ATCC	2.18	>100	2.74	>100	3.48	40.2	0.20	>100
	EKVX	2.83	>100	2.44	32	3.41	41.8	63.10	>100
	HOP-62	2.72	>100	2.22	78.6	8.55	50.5	0.40	>100
	HOP-92	1.61	>100	2.48	>100	5.39	>100	79.43	>100
	NCI-H226	2.15	>100	2.32	>100	4.29	62.7	50.12	>100
	NCI-H23	2.03	>100	2.55	29.4	10.7	64.1	0.32	>100
	NCI-H322M	2.18	>100	2.63	36.2	14.9	>100	0.20	>100
	NCI-H460	1.58	7.64	2.15	9.18	4	36.9	0.06	>100
	NCI-H522	1.59	>100	1.85	57.9	7.82	59.4	7.94	>100
Colon cancer	COLO 205	1.8	—	2.09	7.94	4.8	41.7	0.16	>100
	HCC-2998	1.8	6.03	2.34	19.2	2.93	28.5	0.05	>100
	HCT-116	1.3	6.91	1.43	5.23	1.48	5.41	0.25	25.12
	HCT-15	1.43	>100	1.89	19.5	2.08	26.2	0.10	>100
	HT29	1.7	—	2	11.6	2.32	43.2	0.16	>100
	KM12	1.66	—	1.8	6.05	2.13	12.7	0.20	>100
	SW-620	1.81	—	1.92	8.57	2.17	14.4	1.00	>100
CNS cancer	SF-268	1.88	>100	2.68	40.6	5.05	52.2	1.58	>100
	SF-295	3.03	>100	2.67	31.5	3.98	38.3	0.25	>100
	SF-539	1.63	6.11	1.64	5.7	2.39	23.6	0.06	>100
	SNB-75	1.07	—	1.84	28.6	2.05	30.6	3.98	>100
	U251	1.38	6.41	1.63	7.02	2.18	18.8	1.00	>100
Melanoma	LOX IMVI	1.48	—	1.67	5.79	1.66	6.27	0.25	79.43
	MALME-3M	1.45	—	2.91	32.6	13.9	58.3	0.05	>100
	M14	1.79	—	2.01	9.08	3.5	37.4	1.00	>100
	MDA-MB-435	1.66	—	2.23	16.8	3.46	35.8	0.08	>100
	SK-MEL-2	1.71	8.14	8.66	48.3	11.7	51	63.10	>100
	SK-MEL-28	1.78	—	3.25	34	5.88	42.8	1.00	>100
	SK-MEL-5	1.76	6.12	3.16	32	14	62.7	0.50	79.43
	UACC-257	1.44	—	3.98	70.1	10.1	96.5	3.98	>100
	UACC-62	1.54	6.67	2.76	30.2	6.32	44.1	0.50	>100
	IGROV1	1.9	>100	2	9.77	4.92	40.2	1.26	>100
Ovarian cancer	OVCAR-3	1.69	>100	1.96	7.34	2.75	28	0.02	50.12
	OVCAR-4	1.63	—	3.05	54.2	4.14	39.3	3.98	>100
	OVCAR-5	2.02	>100	1.74	9.07	5.93	43.4	10.00	>100
	OVCAR-8	2.2	>100	3.25	86.5	5.66	>100	1.58	>100
	NCI/ADR-RES	2.32	>100	2.87	>100	5.58	98.8	0.32	>100
	SK-OV-3	3.05	>100	3.82	>100	13.4	87.8	19.95	>100
	786-0	1.76	—	1.65	5.82	2.25	16.6	0.79	>100
Renal cancer	A498	1.32	>100	1.4	35.6	1.67	35.5	0.40	>100
	ACHN	1.95	>100	1.86	8.03	4.81	41.2	0.32	>100
	CAKI-1	2.09	>100	2.54	69.6	5.12	43.4	0.08	>100
	RXF 393	1.46	7.14	1.63	6.53	1.82	9.5	2.51	>100
	SN12C	1.78	>100	2.22	21.6	5.53	41.9	0.50	>100
	UO-31	1.24	—	1.31	5.08	1.75	12.5	1.26	>100
	PC-3	2.14	>100	2.24	>100	2.99	>100	1.58	>100
Prostate cancer	DU-145	1.35	—	2.19	9.56	6.08	43.2	2.51	>100



Table 2 (Contd.)

		Compounds							
		7d		7g		8g		5-FU NS 18893 ^d	
Panel name	Cell name	GI ₅₀ ^a	LC ₅₀ ^b	GI ₅₀	LC ₅₀	GI ₅₀	LC ₅₀	GI ₅₀	LC ₅₀
Breast cancer	MCF7	1.17	6.55	1.25	79.4	1.49	53.7	0.40	>100
	MDA-MB-231/ATCC	2.2	>100	2.69	>100	4.21	40.8	0.08	>100
	HS 578T	1.65	>100	2.61	>100	2.82	>100	6.31	>100
	BT-549	1.35	6.06	1.56	6.11	3.07	30.5	10.00	>100
	T-47D	1.8	>100	2.28	>100	3.4	>100	10.00	>100
	MDA-MB-468	1.34	>100	1.8	8.3	5.54	64.8	7.94	>100

^a GI₅₀ was the drug concentration resulting in a 50% reduction in the net protein increase (as measured by SRB staining) in control cells during the drug incubation, determined at five concentration levels (100, 10, 1.0, 0.1, and 0.01 μM). Italics entries are the most relevant GI₅₀ values of each compound and bold entries are GI₅₀ values (of our compounds) lower than GI₅₀ values of 5-FU. ^b LC₅₀ is a parameter of cytotoxicity that reflects the molar concentration needed to kill 50% of the cells. ^c Data obtained from NCI's *in vitro* disease-oriented human cancer cell lines screen in μM. ^d The values of activity against human cancer cell lines displayed by 5-FU correspond to that reported by. Please visit: <https://dtp.cancer.gov/dtpstandard/cancerscreeningdata/index.jsp>.

while the H-5 proton is observed as a double doublet at 5.63 ppm (with ³J_{MX} = 11.7 Hz and ³J_{AX} = 4.4 Hz), confirming the existence of an AMX coupling system in the pyrazoline ring. In the ¹³C-NMR, the absence of the carbonyl carbon signal and the appearance of signals at 43.3 and 61.6 ppm corresponding to C-4 and C-5, respectively, also confirmed the formation of pyrazolic ring. In general, mass spectra of *N*-(3,5-dichlorophenyl)pyrazolines **9a–g** and **10a–g** show well-defined molecular ion peaks.

It must be highlighted that the synthetic pathway used to obtain the triazine derivatives was efficient, the formation of by-products was not observed, and high yields were achieved. The purity was verified by thin-layer chromatography (TLC), mass spectrometry and proton NMR spectroscopy.

2.2. Anticancer activity evaluation

The *in vitro* anticancer activities of all the synthesized triazine derivatives **5**, **6**, (**7–10**)**a–g** were evaluated by the National Cancer Institute (NCI). Initially, compounds were subjected to preliminary screening at one-dose (10 μM) against 60 human cancer cell lines consisting of nine tumor panels, which include leukemia, lung, colon, melanoma, renal, prostate, CNS, ovarian, and breast cancer cell lines and the results are reported as NCI mean graphs. According to the data analysis of the one-dose mean graphs low GP (growth percent) values indicates better growth inhibition percentages (%GI) (*i.e.* %GI = 100 – GP). The negative GP values correspond to lethal activity, hence, more negative values represent higher activity of the assayed compound. Additionally, low mean values represent better activity and is used as a criteria for further studies. Indeed, mean values ≤ 50 indicate that the compound is active. According to the higher (%GI and lethality) and lower mean values for one-dose criteria, among the evaluated compounds, chalcones **7d**, **7g** and **8g** were actives and displayed the better %GI, lethality and mean values than the remaining assayed compounds, Table 1.

Based on the mean growth data reported in Table 1 and Fig. S1,† it can be observed that:

- The chalcones with substituent R₁ = 4-chloroaniline **8a–g** showed better activity than the respective pyrazolines **10a–g**. This pattern of behavior was not observed in all cases when the substituent was R₁ = morpholine.
- Pyrazolines with substituent R₁ = morpholine showed better activity than those with substituent R₁ = 4-chloroaniline.
- The presence of the 3,4,5-(OCH₃)₃ (R₂ = d) and CF₃ (R₂ = g) groups favor the anticancer properties in both chalcones and pyrazolines, with the exception of chalcone **8d** and pyrazoline **10g**.
- The chalcone **7d** with substituent R₁ = morpholine and R₂ = 3,4,5-(OCH₃)₃ was the leading structure among the series of synthesized compounds, with the best anticancer property.

Due to compounds **7d,g** and **8g** exhibited the broadest spectrum and the highest inhibitory activity among the 30 evaluated compounds against all nine panels of human cancer cell lines at one-dose assay, they were subjected to evaluation at five concentrations of dilution (*i.e.* 100, 10, 1.0, 0.1 and 0.01 μM), in order to determine their antiproliferative activity (GI₅₀ and LC₅₀) (Table 2). Chalcone **7d** showed GI₅₀ values in the range of 0.422–3.05 μM and LC₅₀ values of 6.03 to >100 μM, being the SR cell line (*leukemia*, GI₅₀ = 0.422 μM and LC₅₀ > 100 μM) the most sensitive strain. Compound **7g** exhibited GI₅₀ values in the range of 1.25–8.66 μM and LC₅₀ values of 5.08 to >100 μM, being the MCF7 cell line (*breast cancer*, GI₅₀ = 1.25 μM) the most sensitive strain, while compound **8g** showed GI₅₀ values in the range of 1.48–14.9 μM and LC₅₀ values of 5.41 to >100 μM, being specially effective against the HCT-116 cell line (*colon cancer*) with GI₅₀ = 1.48 μM. The best cytotoxicity value was shown by compound **7g** against UO-31 (*renal cancer*, LC₅₀ = 5.08 μM). Should be noted that compounds **7d,g** and **8g** showed better antiproliferative activity than 5-fluorouracil (5-FU) (standard drug) in several cancer cell lines (Table 2, bold entries).

Additionally, mean GI₅₀ values (per panel) of chalcones **7d,g** and **8g** in comparison with the standard anticancer agent 5-



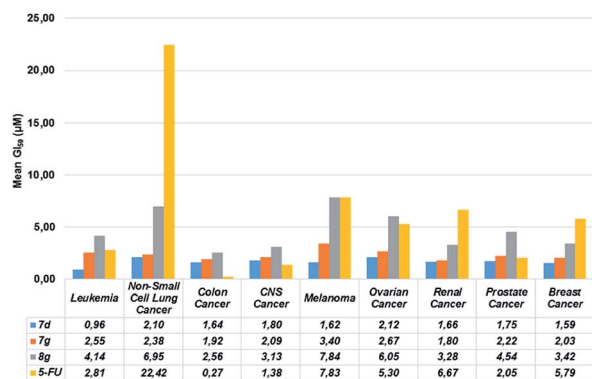


Fig. 2 Comparison of the mean GI_{50} values, per panel, displayed by chalcones **7d**, **7g**, **8g** and the standard drug 5-fluorouracil (5-FU) against the 60 human cancer cell lines.

fluorouracil (5-FU) were determined and drawn in Fig. 2 for a better understanding. Based on these data, chalcone **7d** was more active against all panels of cancer cell lines than compounds **7g** and **8g**, exhibiting lower activity in only two panels of cancer cell lines (*i.e.* colon and CNS) compared to the standard drug 5-FU. Remarkably, chalcone **7d** exhibited the lowest mean GI_{50} value against leukemia panel (0.96 μ M), while

the lowest mean GI_{50} values for compounds **7g** and **8g** were obtained for renal (1.80 μ M) and colon (2.56 μ M) cancer panels, respectively. These finding indicates that compound **7d** might be used as promising lead molecule for discovering a new class of anticancer agents.

2.3. In silico insights

The antiproliferative activities showed by the chalcone and pyrazoline derivatives, lead us to investigate on the suitable biological target that can play a crucial role in the biological response. With this aim molecular modeling protocols, well established in previous works,^{30–33} were applied by using a mixed ligand- and structure-based approach.

The features of the ligand-based approaches supported by molecular descriptors allowed the evaluation of the topological, thermodynamic, and charge-related characteristics of the ligands. Thus, two complementary standpoints in the evaluation of the binding capability (ligand- and structure-based) covered all the interaction aspects in the ligand–target complex.

In the first step the structures were submitted to the web-server DRUDIT (DRUGs Discovery Tools), an open access virtual screening platform, recently developed by us (<https://www.drudit.com>) based on molecular descriptors,³⁴ useful in

Table 3 Biotarget DRUDIT Affinity Scores (DAS) for the studied molecules

Biological target/ cmd	Thymidylate synthase	Serine threonine protein kinase4	Voltage gated sodium channel subunit Nav1-5	Proto-oncogene tyrosine protein kinase Src	Tyrosine protein kinase ZAP-70	Epidermal growth factor receptor EGFR	Nociceptin receptor
5	0.778	0.762	0.812	0.84	0.712	0.702	0.716
6	0.822	0.796	0.81	0.808	0.742	0.786	0.748
7a	0.882	0.846	0.898	0.896	0.886	0.87	0.854
7b	0.894	0.852	0.89	0.9	0.894	0.87	0.88
7c	0.89	0.84	0.9	0.89	0.898	0.874	0.858
7d	0.804	0.754	0.768	0.794	0.85	0.824	0.736
7e	0.882	0.848	0.882	0.872	0.888	0.892	0.834
7f	0.896	0.834	0.888	0.876	0.854	0.874	0.824
7g	0.886	0.768	0.84	0.764	0.776	0.798	0.754
8a	0.874	0.848	0.818	0.846	0.83	0.858	0.8
8b	0.858	0.866	0.83	0.854	0.858	0.876	0.832
8c	0.898	0.856	0.84	0.864	0.872	0.884	0.83
8d	0.84	0.774	0.78	0.782	0.782	0.834	0.734
8e	0.856	0.832	0.766	0.802	0.798	0.832	0.794
8f	0.888	0.836	0.804	0.826	0.8	0.868	0.778
8g	0.878	0.774	0.738	0.724	0.724	0.778	0.74
9a	0.794	0.822	0.81	0.816	0.804	0.816	0.792
9b	0.8	0.822	0.802	0.824	0.788	0.782	0.794
9c	0.786	0.83	0.814	0.81	0.818	0.744	0.798
9d	0.762	0.79	0.748	0.718	0.756	0.668	0.716
9e	0.788	0.82	0.778	0.784	0.788	0.778	0.772
9f	0.808	0.826	0.804	0.81	0.792	0.804	0.802
9g	0.818	0.79	0.736	0.724	0.7	0.646	0.734
10a	0.776	0.822	0.708	0.728	0.754	0.712	0.738
10b	0.768	0.812	0.714	0.728	0.728	0.678	0.748
10c	0.77	0.804	0.714	0.722	0.76	0.68	0.746
10d	0.746	0.764	0.692	0.652	0.704	0.604	0.682
10e	0.756	0.788	0.704	0.694	0.732	0.66	0.724
10f	0.78	0.808	0.722	0.718	0.746	0.69	0.744
10g	0.77	0.756	0.678	0.62	0.616	0.574	0.678
Average	0.825	0.811	0.790	0.790	0.788	0.775	0.773



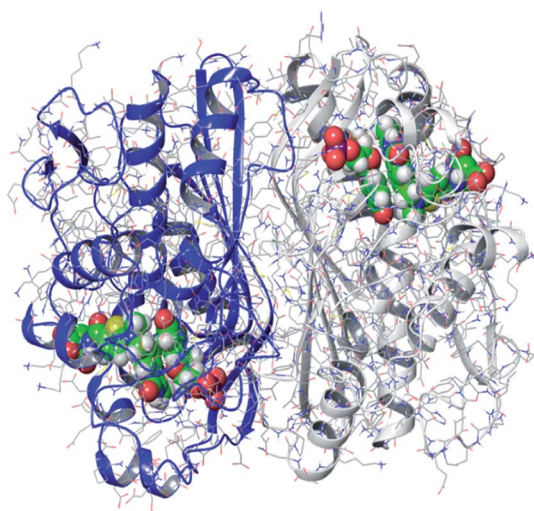


Fig. 3 Thymidylate synthase dimer (from PDB ID 5X5Q).

the identification of suitable biological targets for small molecules.

In particular, by the Biotarget Predictor tool, the DRUDIT Affinity Score (DAS) is assigned to each input structure *versus*

Table 4 IFD results for precursors **5**, **6**, chalcones (**7,8**)a–g and *N*-(3,5-dichlorophenyl)pyrazolines (**9,10**)a–g

Cmd	Docking XP score	IFD score
5	-9.485	-589.383
6	-12.496	-591.632
7a	-9.645	-594.712
7b	-13.681	-597.86
7c	-13.301	-595.368
7d	-12.161	-598.947
7e	-12.382	-596.397
7f	-10.889	-594.444
7g	-12.672	-597.106
8a	-12.765	-592.985
8b	-13.461	-598.765
8c	-11.157	-597.44
8d	-11.701	-596.742
8e	-12.406	-594.546
8f	-12.018	-593.787
8g	-15.116	-598.53
9a	-12.401	-597.581
9b	-11.993	-597.761
9c	-11.898	-597.398
9d	-9.545	-593.173
9e	-14.838	-601.736
9f	-13.206	-599.526
9g	-12.101	-598.997
10a	-13.657	-600.72
10b	-9.9	-600.609
10c	-15.252	-599.967
10d	-11.00	-589.16
10e	-11.842	-598.052
10f	-13.633	-598.584
10g	-11.598	-591.941
Raltitrexed	-13.828	-584.621

the biological targets database implemented in the tool. The DAS values of the molecules under investigation against the best biological targets are reported in Table 3.

The obtained results showed as the molecules under investigation have a quite good affinity against thymidylate synthase (TS) (DAS averaged 0.825, which reaches 0.87 for the derivatives **7** and **8**), thus to get information on which molecular features are involved in the binding, structure-based studies were performed.

The monomer of TS consists of an α/β -fold containing 7 α -helices and 10 β -strands, arranged in three layers: a six stranded mixed β -sheet, a long α -helix across the sheet flanked by two shorter helices, and a mixed layer containing two antiparallel two stranded β -sheets and the remaining four helices. The large β -sheets from the monomers stack against each other to form the dimer interface (Fig. 3). The dimer has two active sites, one within each monomer. In this study, the monomer was extracted from the high-resolution crystal structure of TS (PDB ID: 5X5Q)³⁵ downloaded from the Protein Databank (<https://www.rcsb.org>).³⁶

With the aim to confirm the ligand-based results, to investigate the structural interactions, and to predict the binding poses within the human thymidylate synthase binding site, all the synthesized molecules were processed by Induced Fit Docking (IFD) calculations.

The IFD results on chalcone- and pyrazoline-based 1,3,5-triazine derivatives confirmed the ligand-based evidence. In particular, the most active compounds (**7d,g** and **8g**) showed

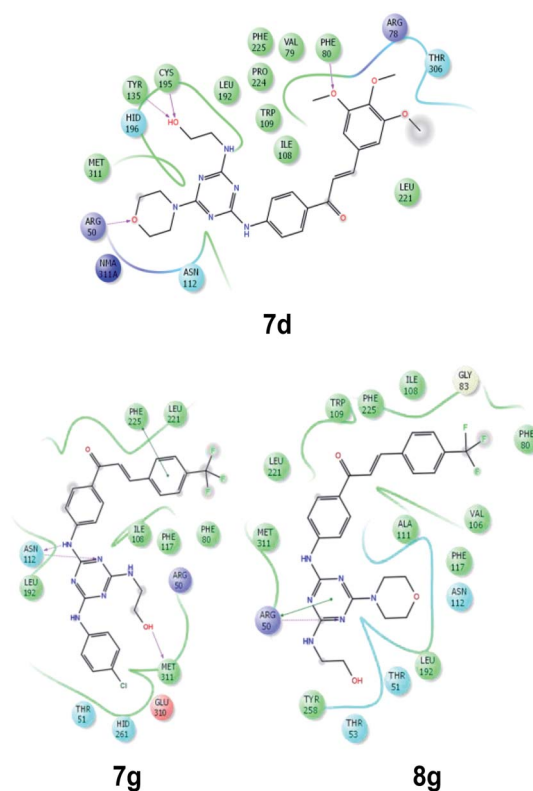


Fig. 4 Amino acid maps representations of the best scored derivatives (7d,g and 8g).

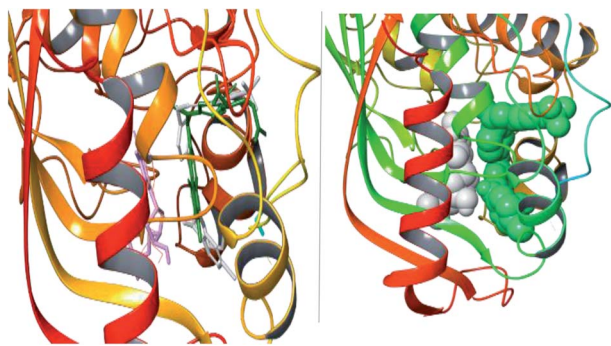


Fig. 5 Left: superposition of **8g** (white) and raltitrexed (green). Right: stacking interaction between **8g** (green) and UMP (white).

excellent docking scores, comparable to reference compound raltitrexed (Table 4). The derivatives **9e** and **10c** showed the higher scores, although the *in wet* results and the ligand based outputs not classified them as TS modulators. It is conceivable that, although the molecular structures well fit TS active site, other chemical-physical properties do not contribute to overall affinity.

The analysis of the amino acid maps of the most active compounds (**7d,g** and **8g**), confirmed as they interact with the pivotal amino acid residues (Arg50, Leu 108, Asn112, Leu192, Leu221, Phe225, and Met311), which have a central role in the catalytic enzyme process of the TS (Fig. 4).

As seen from 3D docking representation of the **8g** derivative the core occupies the same binding site as does the reference ligand (Fig. 5, left) and makes stacking interaction with pyrimidine ring of UMP (Fig. 5, right). This stacking interaction is crucial and has been conserved in all the thymidylate synthases for with crystal structures that have been solved in complex with the cofactor and the inhibitor.

The overall results are in agreement with the hypothesis that the antiproliferative activities are related to the capability of these structures to modulate the TS, although, they could involve other biological targets as suggested from the ligand-based results (Table 3).

3. Conclusions

In this study, novel chalcone- and pyrazoline-based 1,3,5-triazines were synthesized using a versatile methodology, achieving high yields and purity. These triazine derivatives were evaluated for their anticancer effects on nine panels of 60 human cancer cell lines. Compounds **7d,g** and **8g** exhibited significant antiproliferative activity on all cancer panels being specially effective against the SR leukemia cell line, MCF7 breast cancer cell line and HCT-116 colon cancer cell line, respectively, and furthermore showed better GI₅₀ values than 5-FU against several cell lines. Compound **7d** exhibited the lowest mean GI₅₀ against all panels of cancer cell lines and showed excellent docking score, comparable to reference compound raltitrexed. According to these results, chalcone **7d** (R_1 = morpholine, R_2 = 3,4,5-(OCH₃)₃) could be considered as promising leads for further development of more potent anticancer agents.

4. Experimental section

4.1. General information

Reagents and solvents used were obtained from commercial sources and used without further purification. Melting points were measured using a Stuart SMP10 melting point device (Cole-Parmer Ltd, Stone, Staffordshire, UK) and are uncorrected. FTIR spectra were obtained with a IRAffinity-1 spectrophotometer (Shimadzu, Columbia, MD, USA). The ¹H- and ¹³C-NMR spectra were run on a DPX 400 spectrometer (Bruker, Billerica, MA, USA) operating at 400 and 100 MHz respectively, using DMSO-*d*₆ as solvent and TMS as internal standard. The mass spectra were obtained on a Shimadzu-GCMS-QP2010 spectrometer (Shimadzu, Kyoto, Honshu, Japan) operating at 70 eV. The elemental analyses were obtained using an Agilent CHNS elemental analyzer (Thermo Fischer Scientific Inc., Madison, WI, USA) and the values are within ±0.4% of the theoretical values. Thin layer chromatography (TLC) were performed on 0.2 mm pre-coated aluminium plates of silica gel 60 F254 (Merck, Darmstadt, Hesse, Germany).

4.2. Chemistry

4.2.1. General procedure for synthesis of 1-4-((4,6-dichloro-1,3,5-triazin-2-yl)amino)phenyl)ethan-1-one (2). Using a methodology similar to that reported by Kathiriya³⁷ and coworkers, the synthesis of precursor **2** was carried out as follows: a mixture of 2,4,6-trichloro-1,3,5-triazine **1** (0.027 mol, 1 equiv.) and 4-aminoacetophenone (0.027 mol, 1 equiv.) in acetone (25 mL) was stirred at −5–0 °C for 5 h. The mixture was neutralized with 20% Na₂CO₃. The content was poured onto crushed ice, filtered and washed with water.

4.2.2. General procedure for synthesis of 1-4-((4-chloro-6-morpholino-1,3,5-triazin-2-yl)amino)phenyl)ethan-1-one (3). A mixture of ketone **2** (0.014 mmol, 1.2 equiv.) and morpholine (0.012 mol, 1 equiv.) in acetone (25 mL) was stirred at −5–0 °C for 6 h. The mixture was neutralized with 20% Na₂CO₃. The content was poured onto crushed ice, filtered and washed with water. No further purification was required.

4.2.2.1. 1-4-((4-Chloro-6-morpholino-1,3,5-triazin-2-yl)amino)phenyl)ethan-1-one (3). White solid; 70% yield; mp 218–220 °C. FT-IR (ATR) ν (cm^{−1}) 3316 (N–H), 3117 (=C–H), 1659 (C=O), 1578 and 1516 (C=N and C=C). ¹H-NMR (400 MHz, DMSO-*d*₆) δ ppm 2.50 (s, 3H, CH₃), 3.44–3.81 (m, 8H, CH₂), 7.76 (d, J = 8.8 Hz, 2H, Ar–H), 7.90 (d, J = 8.8 Hz, 2H, Ar–H), 10.36 (bs, 1H, NH). ¹³C-NMR (100 MHz, DMSO-*d*₆) δ ppm 26.4 (CH₃), 43.4 (CH₂), 59.15 (CH₂), 119.1 (CH), 129.3 (CH), 131.1 (Cq), 143.5 (Cq), 143.7 (Cq), 165.5 (Cq), 167.9 (Cq), 196.4 (Cq). MS (70 eV) m/z (%): 333 (11), 282 (23), 267 (100), 170 (26), 145 (44), 90 (32). Anal. calcd C₁₅H₁₆ClN₅O₂: C, 53.98; H, 4.83; N, 20.98; found: C, 54.01; H, 4.86; N, 20.70.

4.2.3. General procedure for synthesis of 1-4-((4-chloro-6-((4-chlorophenyl)amino)-1,3,5-triazin-2-yl)amino)phenyl)ethan-1-one (4). A mixture of ketone **2** (0.011 mol, 1 equiv.) and 4-chloroaniline (0.011 mol, 1 equiv.) in dioxane (25 mL) was stirred at room temperature for 12 h. The mixture was neutralized with 20% Na₂CO₃. The content was poured onto



crushed ice, filtered and washed with water. No further purification was required.

4.2.3.1. 1-(4-((4-Chloro-6-((4-chlorophenyl)amino)-1,3,5-triazin-2-yl)amino)phenyl)ethan-1-one (4). White solid; 80% yield; mp 258–260 °C. FT-IR (ATR) ν (cm⁻¹) 3267 (N–H), 3101 (=C–H), 1666 (C=O), 1566 and 1512 (C=N and C=C). ¹H-NMR (400 MHz, DMSO-*d*₆) δ ppm 2.54 (s, 3H, CH₃), 7.42 (d, *J* = 8.8 Hz, 2H, Ar–H), 7.62–7.89 (m, 4H, Ar–H), 7.93 (d, *J* = 8.8 Hz, 2H, Ar–H), 10.48 (bs, 2H, NH). ¹³C-NMR (100 MHz, DMSO-*d*₆) δ ppm 26.5 (CH₃), 119.8 (CH), 122.5 (CH), 127.4 (Cq), 128.5 (CH), 129.2 (CH), 131.6 (Cq), 137.3 (Cq), 143.0 (Cq), 163.8 (Cq), 168.3 (Cq), 168.4 (Cq), 196.5 (Cq). MS (70 eV) *m/z* (%): 373 : 375 : 377 [M^+] : [$M + 2$]⁺ : [$M + 4$]⁺ (90/59/11), 358 (75), 222 (10), 179 (16), 145 (100), 90 (27). Anal. calcd C₁₇H₁₃Cl₂N₅O: C, 54.56; H, 3.50; N, 18.71; found: C, 54.01; H, 3.55; N, 18.74.

4.2.4. General procedure for synthesis of 1-(4-((2-hydroxyethyl)amino)-6-morpholino-1,3,5-triazin-2-yl)amino)phenyl)ethan-1-one (5). A mixture of disubstituted triazine 3 (0.006 mol, 1 equiv.) and ethanolamine (0.018 mol, 3 equiv.) in dioxane (20 mL) was stirred at reflux for 8 h. The mixture was neutralized with 20% Na₂CO₃. The content was poured onto crushed ice, filtered and washed with water. No further purification was required.

4.2.4.1. 1-(4-((4-((2-Hydroxyethyl)amino)-6-morpholino-1,3,5-triazin-2-yl)amino)phenyl)ethan-1-one (5). White solid. 76% yield; mp 191–193 °C. FT-IR (ATR): ν (cm⁻¹) 3350 (N–H), 3279 (O–H), 3093 (=C–H), 1668 (C=O), 1583 and 1537 (C=N and C=C). ¹H-NMR (400 MHz, DMSO-*d*₆) δ ppm 2.52 (s, 3H, CH₃), 3.32–3.42 (m, 2H, CH₂), 3.50–3.57 (m, 2H, CH₂), 3.57–3.63 (m, 4H, CH₂), 3.66–3.74 (m, 4H, CH₂), 4.80 (s, 1H, OH), 6.88 (bs, 1H, NH), 7.83–7.90 (m, 4H, Ar–H), 9.39 (bs, 1H, NH). ¹³C-NMR (100 MHz, DMSO-*d*₆) δ ppm 26.5 (CH₃), 43.0 (CH₂), 43.6 (CH₂), 60.2 (CH₂), 66.2 (CH₂), 118.6 (CH), 129.5 (CH), 130.1 (Cq), 145.4 (Cq), 165.0 (Cq), 165.9 (Cq), 166.1 (Cq), 196.9 (Cq). MS (70 eV) *m/z* (%): 358 [M^+] (32), 328 (59), 313 (43), 69 (36), 55 (54), 43 (100). Anal. calcd C₁₇H₂₂N₆O₃: C, 56.97; H, 6.19; N, 23.45; found: C, 57.00; H, 6.25; N, 23.60.

4.2.5. General procedure for synthesis of 1-(4-((4-(4-chlorophenyl)amino)-6-((2-hydroxyethyl)amino)-1,3,5-triazin-2-yl)amino)phenyl)ethan-1-one (6). A mixture of disubstituted triazine 4 (0.005 mol, 1 equiv.) and ethanolamine (0.016 mol, 3 equiv.) in dioxane (20 mL) was stirred at reflux for 8 h. The mixture was neutralized with 20% Na₂CO₃. The content was poured onto crushed ice, filtered and washed with water. No further purification was required.

4.2.5.1. 1-(4-((4-((4-Chlorophenyl)amino)-6-((2-hydroxyethyl)amino)-1,3,5-triazin-2-yl)amino)phenyl)ethan-1-one (6). White solid. 78% yield; mp 160–163 °C. FT-IR (ATR): ν (cm⁻¹) 3398 (N–H), 3284 (O–H), 3113 (=C–H), 1666 (C=O), 1589 y 1566 (C=N and C=C). ¹H-NMR (400 MHz, DMSO-*d*₆) δ ppm 2.54 (s, 3H, CH₃), 3.45 (bs, 2H, CH₂), 3.59 (t, *J* = 5.6 Hz, 2H, CH₂), 4.12 (s, 1H, OH), 7.39 (d, *J* = 8.2 Hz, 2H, Ar–H), 7.75 (d, *J* = 8.2 Hz, 2H, Ar–H), 7.84–7.94 (m, 4H, Ar–H), 8.24 (bs, 1H, NH), 10.15–10.55 (m, 2H, NH). ¹³C-NMR (100 MHz, DMSO-*d*₆) δ ppm 26.5 (CH₃), 43.3 (CH₂), 59.4 (CH₂), 119.9 (CH), 122.4 (CH), 122.9 (Cq), 128.5 (CH), 129.2 (CH), 131.4 (Cq), 131.5 (Cq), 143.2 (Cq), 158.7 (Cq), 161.0 (Cq), 161.2 (Cq), 196.5 (Cq). MS (70 eV) *m/z* (%): 398 : 400

[M^+] : [$M + 2$]⁺ (65/23), 367 (98), 353 (92), 296 (36), 176 (42), 145 (45), 57 (38), 43 (100). Anal. calcd C₁₉H₁₉ClN₆O₂: C, 57.22; H, 4.80; N, 21.07; found: C, 57.19; H, 4.83; N, 21.10.

4.2.6. General procedure for synthesis of 1-(4-((4-((2-hydroxyethyl)amino)-6-morpholino-1,3,5-triazin-2-yl)amino)phenyl)chalcones (7a–g). A mixture of ketone 5 (1 equiv.), the respective benzaldehyde (1.2 equiv.) and potassium hydroxide (100 mg) in ethanol (2.5 mL) was stirred at room temperature for 5 h. The solid formed was filtered and washed with ethanol. No further purification was required.

4.2.6.1. (E)-1-(4-((4-((2-Hydroxyethyl)amino)-6-morpholino-1,3,5-triazin-2-yl)amino)phenyl)-3-phenylprop-2-en-1-one (7a). Yellow solid. 75% yield; mp 175–177 °C. FT-IR (ATR): ν (cm⁻¹) 3400 (N–H), 3315 (O–H), 3120 (=C–H), 1657 (C=O), 1576 y 1533 (C=N and C=C). ¹H-NMR (400 MHz, DMSO-*d*₆) δ ppm 3.31–3.47 (m, 2H, CH₂), 3.49–3.57 (m, 2H, CH₂), 3.59–3.67 (m, 4H, CH₂), 3.68–3.76 (m, 4H, CH₂), 4.76 (s, 1H, OH), 6.99 (t, *J* = 5.0 Hz, 1H, NH), 7.42–7.48 (m, 3H, Ar–H), 7.70 (d, *J* = 15.6 Hz, 1H, CH), 7.87 (d, *J* = 4.8 Hz, 2H, Ar–H), 7.91–8.01 (m, 3H, Ar–H, CH), 8.11 (t, *J* = 10.0 Hz, 2H, Ar–H), 9.53 (bs, 1H, NH). ¹³C-NMR (100 MHz, DMSO-*d*₆) δ ppm 43.0 (CH₂), 43.4 (CH₂), 60.0 (CH₂), 66.1 (CH₂), 114.6 (Cq), 118.4 (CH), 122.1 (CH), 128.8 (CH), 128.9 (CH), 129.8 (Cq), 129.9 (CH), 130.4 (CH), 134.9 (Cq), 142.9 (CH), 164.1 (Cq), 164.8 (Cq), 165.6 (Cq), 187.3 (Cq). MS (70 eV) *m/z* (%): 446 [M^+] (19), 416 (17), 401 (12), 131 (27), 103 (37), 69 (60), 55 (86). Anal. calcd C₂₄H₂₆N₆O₃: C, 64.56; H, 5.87; N, 18.82; found: C, 64.60; H, 5.90; N, 18.79.

4.2.6.2. (E)-1-(4-((4-((2-Hydroxyethyl)amino)-6-morpholino-1,3,5-triazin-2-yl)amino)phenyl)-3-(p-tolyl)prop-2-en-1-one (7b). Yellow solid. 68% yield; mp 185–191 °C. FT-IR (ATR): ν (cm⁻¹) 3419 (N–H), 3291 (O–H), 3110 (=C–H), 1651 (C=O), 1585 y 1537 (C=N and C=C). ¹H-NMR (400 MHz, DMSO-*d*₆) δ ppm 2.35 (s, 3H, CH₃), 3.26–3.47 (m, 2H, CH₂), 3.54 (q, *J* = 6.1 Hz, 2H, CH₂), 3.59–3.66 (m, 4H, CH₂), 3.67–3.75 (m, 4H, CH₂), 4.74 (s, 1H, OH), 6.98 (t, *J* = 5.6 Hz, 1H, NH), 7.26 (d, *J* = 8.0 Hz, 2H, Ar–H), 7.67 (d, *J* = 15.2 Hz, 1H, CH), 7.77 (d, *J* = 8.0 Hz, 2H, Ar–H), 7.85–7.98 (m, 3H, Ar–H, CH), 8.10 (t, *J* = 9.8 Hz, 2H, Ar–H), 9.51 (bs, 1H, NH). ¹³C-NMR (100 MHz, DMSO-*d*₆) δ ppm 21.1 (CH₃), 42.9 (CH₂), 43.4 (CH₂), 59.9 (CH₂), 66.1 (CH₂), 118.4 (CH), 121.0 (CH), 128.8 (CH), 128.9 (Cq), 129.2 (Cq), 129.6 (CH), 129.8 (CH), 132.2 (Cq), 140.4 (Cq), 143.0 (CH), 164.6 (Cq), 164.8 (Cq), 165.9 (Cq), 187.3 (Cq). MS (70 eV) *m/z* (%): 460 [M^+] (12), 430 (10), 145 (23), 117 (15), 69 (58), 55 (78), 43 (100). Anal. calcd C₂₅H₂₈N₆O₃: C, 65.20; H, 6.13; N, 18.25; found: C, 65.18; H, 6.18; N, 18.19.

4.2.6.3. (E)-1-(4-((4-((2-Hydroxyethyl)amino)-6-morpholino-1,3,5-triazin-2-yl)amino)phenyl)-3-(4-methoxyphenyl)prop-2-en-1-one (7c). Yellow solid. 83% yield; mp 179–183 °C. FT-IR (ATR): ν (cm⁻¹) 3479 (N–H), 3277 (O–H), 3201 (=C–H), 1649 (C=O), 1571 y 1506 (C=N and C=C). ¹H-NMR (400 MHz, DMSO-*d*₆) δ ppm 3.38–3.41 (m, 2H, CH₂), 3.53 (q, *J* = 6.2 Hz, 2H, CH₂), 3.60–3.67 (m, 4H, CH₂), 3.67–3.75 (m, 4H, CH₂), 3.81 (s, 3H, OCH₃), 4.76 (s, 1H, OH), 6.94–7.04 (m, 3H, NH, Ar–H), 7.67 (d, *J* = 15.6 Hz, 1H, CH), 7.77–7.86 (m, 3H, Ar–H, CH), 7.94 (d, *J* = 7.2 Hz, 2H, Ar–H), 8.09 (t, *J* = 9.8 Hz, 2H, Ar–H), 9.50 (bs, 1H, NH). ¹³C-NMR (100 MHz, DMSO-*d*₆) δ ppm 43.0 (CH₂), 43.3 (CH₂), 55.4 (CH₃), 59.9 (CH₂), 66.0 (CH₂), 114.4 (CH), 118.4 (CH), 119.6 (CH), 127.5 (Cq), 129.6 (CH), 130.6 (CH), 142.8 (CH), 161.2 (Cq), 164.1 (Cq), 164.2 (Cq), 164.8 (Cq), 165.9 (Cq), 165.9 (Cq), 187.2 (Cq). MS (70 eV) *m/z* (%): 476 [M^+] (6), 446



(5), 161 (7), 98 (12), 83 (19), 69 (40), 55 (61), 43 (100). Anal. calcd $C_{25}H_{28}N_6O_4$: C, 63.01; H, 5.92; N, 17.64; found: C, 62.99; H, 5.93; N, 17.60.

4.2.6.4. (E)-1-(4-((4-((2-Hydroxyethyl)amino)-6-morpholino-1,3,5-triazin-2-yl)amino)phenyl)-3-(3,4,5-trimethoxyphenyl)prop-2-en-1-one (7d). Yellow solid. 87% yield; mp 218–224 °C. FT-IR (ATR): ν (cm^{-1}) 3354 (N–H), 3267 (O–H), 3100 (C–H), 1649 (C=O), 1587 y 1537 (C=N and C=C). 1H -NMR (400 MHz, DMSO- d_6) δ ppm 3.36–3.40 (m, 2H, CH₂), 3.53 (q, J = 5.7 Hz, 2H CH₂), 3.60–3.67 (m, 4H, CH₂), 3.68–3.75 (m, 7H, CH₂, OCH₃), 3.87 (s, 6H, OCH₃), 4.73 (s, 1H, OH), 6.98 (t, J = 6.0 Hz, 1H, NH), 7.2 (s, 2H, Ar–H), 7.66 (d, J = 15.2 Hz, 1H, CH), 7.82–8.02 (m, 3H, Ar–H, CH), 8.13 (t, J = 9.6 Hz, 2H, Ar–H), 9.52 (bs, 1H, NH). ^{13}C -NMR (100 MHz, DMSO- d_6) δ ppm 42.9 (CH₂), 43.4 (CH₂), 56.2 (CH₃), 59.8 (CH₂), 60.2 (CH₃), 66.1 (CH₂), 106.4 (CH), 118.4 (CH), 121.2 (CH), 129.7 (CH), 129.8 (CH), 130.5 (Cq), 139.5 (Cq), 143.3 (Cq), 145.4 (Cq), 153.1 (Cq), 165.6 (Cq), 165.7 (Cq), 165.8 (Cq), 187.2 (Cq). MS (70 eV) m/z (%): 536 [M^+] (15), 505 (10), 491 (8), 475 (6), 461 (11), 145 (18), 69 (58), 55 (71). Anal. calcd $C_{27}H_{32}N_6O_6$: C, 60.47; H, 5.98; N, 15.68; found: C, 60.44; H, 6.01; N, 15.66.

4.2.6.5. (E)-3-(4-Chlorophenyl)-1-(4-((4-((2-hydroxyethyl)amino)-6-morpholino-1,3,5-triazin-2-yl)amino)phenyl)prop-2-en-1-one (7e). Yellow solid. 92% yield; mp 200–205 °C. FT-IR (ATR): ν (cm^{-1}) 3400 (N–H), 3294 (O–H), 3100 (C–H), 1657 (C=O), 1572 y 1541 (C=N and C=C). 1H -NMR (400 MHz, DMSO- d_6) δ ppm 3.38–3.40 (m, 2H, CH₂), 3.53 (q, J = 6.3 Hz, 2H, CH₂), 3.60–3.66 (m, 4H, CH₂), 3.76–3.67 (m, 4H, CH₂), 4.76 (s, 1H, OH), 7.00 (t, J = 5.9 Hz, 1H, NH), 7.52 (d, J = 8.4 Hz, 2H, Ar–H), 7.68 (d, J = 15.6 Hz, 1H, CH), 7.89–7.99 (m, 5H, Ar–H, CH), 8.11 (t, J = 10.0 Hz, 2H, Ar–H), 9.54 (bs, 1H, NH). ^{13}C -NMR (100 MHz, DMSO- d_6) δ ppm 42.9 (CH₂), 43.4 (CH₂), 60.0 (CH₂), 66.0 (CH₂), 118.4 (CH), 122.9 (Cq), 129.0 (CH), 129.8 (CH), 129.9 (CH), 130.5 (CH), 130.9 (Cq), 133.9 (Cq), 134.9 (Cq), 141.4 (CH), 164.1 (Cq), 164.6 (Cq), 165.9 (Cq), 187.1 (Cq). MS (70 eV) m/z (%): 480 : 482 [M^+] : [$M + 2$]⁺ (12/4), 449 (14), 437 (12), 165 (16), 145 (16), 137 (18), 102 (17), 69 (61), 55 (92). Anal. calcd $C_{24}H_{25}ClN_6O_3$: C, 59.94; H, 5.24; N, 17.47; found: C, 60.01; H, 5.19; N, 17.53.

4.2.6.6. (E)-3-(4-Fluorophenyl)-1-(4-((4-((2-hydroxyethyl)amino)-6-morpholino-1,3,5-triazin-2-yl)amino)phenyl)prop-2-en-1-one (7f). Yellow solid. 80% yield; mp 198–204 °C. FT-IR (ATR): ν (cm^{-1}) 3400 (N–H), 3278 (O–H), 3100 (C–H), 1649 (C=O), 1579 y 1541 (C=N and C=C). 1H -NMR (400 MHz, DMSO- d_6) δ ppm 3.31–3.38 (m, 2H, CH₂), 3.48–3.58 (m, 2H, CH₂), 3.60–3.67 (m, 4H, CH₂), 3.68–3.76 (m, 4H, CH₂), 4.77 (s, 1H, OH), 7.00 (t, J = 4.8 Hz, 1H, NH), 7.30 (t, J_{HF} = 8.8 Hz, 2H, Ar–H), 7.70 (d, J = 15.6 Hz, 1H, CH), 7.84–8.01 (m, 5H, Ar–H, CH), 8.11 (t, J = 10.2 Hz, 2H, Ar–H), 9.53 (bs, 1H, NH). ^{13}C -NMR (100 MHz, DMSO- d_6) δ ppm 42.9 (CH₂), 43.4 (CH₂), 60.1 (CH₂), 66.0 (CH₂), 115.9 (d, $^2J_{CF}$ = 22.0 Hz, (CH)), 118.4 (CH), 122.1 (CH), 129.8 (CH), 131.1 (d, $^3J_{CF}$ = 9.0 Hz, (CH)), 131.6 (d, $^4J_{CF}$ = 3.1 Hz, Cq), 139.2 (Cq), 141.6 (CH), 162.1 (Cq), 164.6 (Cq), 165.7 (Cq), 167.0 (Cq), 173.8 (d, $^1J_{C-F}$ = 241.6 Hz, Cq), 187.2 (Cq). MS (70 eV) m/z (%): 464 (1), 256 (1), 185 (1), 97 (8), 73 (33), 69 (57), 55 (56). Anal. calcd. $C_{24}H_{25}FN_6O_3$: C, 62.06; H, 5.43; N, 18.09; found: C, 62.10; H, 5.38; N, 18.09.

4.2.6.7. (E)-1-(4-((4-((2-Hydroxyethyl)amino)-6-morpholino-1,3,5-triazin-2-yl)amino)phenyl)-3-(4-(trifluoromethyl)phenyl)prop-2-en-1-one (7g). Yellow solid. 76% yield; mp 227–230 °C. FT-IR (ATR): ν

(cm^{-1}) 3415 (N–H), 3277 (O–H), 3211 (C–H), 1651 (C=O), 1577 y 1535 (C=N and C=C). 1H -NMR (400 MHz, DMSO- d_6) δ ppm 3.42–3.20 (m, 2H, CH₂), 3.48–3.56 (m, 2H, CH₂), 3.59–3.66 (m, 4H, CH₂), 3.69–3.76 (m, 4H, CH₂), 4.80 (s, 1H, OH), 7.04 (bs, 1H, NH), 7.75 (d, J = 14.0 Hz, 1H, CH), 7.80 (d, J = 8.4 Hz, 2H, Ar–H), 8.02–7.92 (m, 2H, Ar–H), 8.19–8.07 (m, 5H, Ar–H, CH), 9.58 (bs, 1H, NH). ^{13}C -NMR (100 MHz, DMSO- d_6) δ ppm 43.0 (CH₂), 43.4 (CH₂), 59.9 (CH₂), 66.1 (CH₂), 118.5 (CH), 124.1 (q, $^1J_{CF}$ = 245.9 Hz, CF₃), 124.9 (CH), 125.8 (CH), 129.5 (q, $^3J_{CF}$ = 16.7 Hz, (CH)), 130.1 (CH), 139.0 (Cq), 139.7 (Cq), 141.0 (CH), 145.8 (Cq), 146.2 (Cq), 164.0 (Cq), 164.2 (Cq), 165.3 (q, $^2J_{CF}$ = 24.6 Hz, Cq), 187.3 (Cq). MS (70 eV) m/z (%): 514 (6), 484 (8), 469 (6), 199 (8), 145 (13), 69 (58), 55 (83). Anal. calcd $C_{25}H_{25}F_3N_6O_3$: C, 58.36; H, 4.90; N, 16.33; found: C, 58.40; H, 5.00; N, 16.30.

4.2.7. General procedure for synthesis of 1-(4-((4-((4-chlorophenyl)amino)-6-((2-hydroxyethyl)amino)-1,3,5-triazin-2-yl)amino)phenyl)chalcones (8a–g). A mixture of ketone **6** (1 equiv.), the respective benzaldehyde (1.2 equiv.) and potassium hydroxide (100 mg) in ethanol (2.5 mL) was stirred at room temperature for 5 h. The solid formed was filtered and washed with ethanol. No further purification was required.

4.2.7.1. (E)-1-(4-((4-((4-Chlorophenyl)amino)-6-((2-hydroxyethyl)amino)-1,3,5-triazin-2-yl)amino)phenyl)-3-phenylprop-2-en-1-one (8a). Yellow solid. 88% yield; mp 192–206 °C. FT-IR (ATR): ν (cm^{-1}) 3400 (N–H), 3292 (O–H), 3119 (C–H), 1637 (C=O), 1572 y 1558 (C=N and C=C). 1H -NMR (400 MHz, DMSO- d_6) δ ppm 3.36–3.48 (m, 2H, CH₂), 3.53–3.63 (m, 2H, CH₂), 4.78 (s, 1H, OH), 7.17 (bs, 1H, NH), 7.28–7.34 (m, 2H, Ar–H), 7.46 (d, J = 5.2 Hz, 2H, Ar–H), 7.71 (d, J = 15.6 Hz, 1H, CH), 7.81–7.89 (m, 4H, Ar–H, CH), 7.90–7.98 (m, 2H, Ar–H), 8.03 (d, J = 8.4 Hz, 2H, Ar–H), 8.11 (t, J = 8.4 Hz, 2H, Ar–H), 9.33 (bs, 1H, NH), 9.57 (bs, 1H, NH). ^{13}C -NMR (100 MHz, DMSO- d_6) δ ppm 43.0 (CH₂), 59.8 (CH₂), 118.8 (CH), 121.4 (CH), 122.2 (CH), 125.3 (Cq), 125.4 (Cq), 128.2 (CH), 128.7 (CH), 128.9 (CH), 129.6 (CH), 130.4 (CH), 134.0 (Cq), 134.9 (Cq), 139.2 (Cq), 142.9 (CH), 163.8 (Cq), 164.0 (Cq), 165.7 (Cq), 187.4 (Cq). MS (70 eV) m/z (%): 486 : 488 [M^+] : [$M + 2$]⁺ (50/24), 456 (49), 443 (43), 178 (48), 145 (44), 131 (65), 103 (100), 77 (39). Anal. calcd $C_{26}H_{23}ClN_6O_2$: C, 64.13; H, 4.76; N, 17.26; found: C, 64.17; H, 4.80; N, 17.23.

4.2.7.2. (E)-1-(4-((4-((4-Chlorophenyl)amino)-6-((2-hydroxyethyl)amino)-1,3,5-triazin-2-yl)amino)phenyl)-3-(p-tolyl)prop-2-en-1-one (8b). Yellow solid. 85% yield; mp 219–224 °C. FT-IR (ATR): ν (cm^{-1}) 3543 (N–H), 3294 (O–H), 3119 (C–H), 1616 (C=O), 1583 y 1531 (C=N and C=C). 1H -NMR (400 MHz, DMSO- d_6) δ ppm 2.35 (s, 3H, CH₃), 3.41–3.48 (m, 2H, CH₂), 3.54–3.62 (m, 2H, CH₂), 4.70 (bs, 1H, OH), 7.13 (bs, 1H, NH), 7.35–7.22 (m, 4H, Ar–H), 7.68 (d, J = 15.6 Hz, 1H, CH), 7.76 (d, J = 7.6 Hz, 2H, Ar–H), 7.81–7.91 (m, 3H, Ar–H, CH), 8.00 (d, J = 8.4 Hz, 2H, Ar–H), 8.09 (t, J = 7.2 Hz, 2H, Ar–H), not observed NH. ^{13}C -NMR (100 MHz, DMSO- d_6) δ ppm 21.1 (CH₃), 43.1 (CH₂), 59.9 (CH₂), 118.8 (CH), 121.2 (CH), 121.4 (CH), 125.3 (Cq), 128.2 (CH), 128.8 (CH), 129.6 (CH), 129.6 (CH), 130.7 (Cq), 132.2 (Cq), 139.3 (Cq), 140.4 (Cq), 143.0 (CH), 145.4 (Cq), 163.9 (Cq), 164.1 (Cq), 165.8 (Cq), 187.4 (Cq). MS (70 eV) m/z (%): 500 : 502 [M^+] : [$M + 2$]⁺ (5/3), 367 (10), 353 (9), 149 (12), 119 (22), 91 (33), 81 (31). Anal. calcd $C_{27}H_{25}ClN_6O_2$: C, 64.73; H, 5.03; N, 16.78; found: C, 64.70; H, 4.99; N, 16.80.

4.2.7.3. (E)-1-(4-((4-((4-Chlorophenyl)amino)-6-((2-hydroxyethyl)amino)-1,3,5-triazin-2-yl)amino)phenyl)-3-(4-methoxyphenyl)prop-2-



en-1-one (8c). Yellow solid. 75% yield; mp 210–214 °C. FT-IR (ATR): ν (cm⁻¹) 3400 (N–H), 3277 (O–H), 3117 (=C–H), 1637 (C=O), 1576 γ 1558 (C=N and C=C). ¹H-NMR (400 MHz, DMSO-*d*₆) δ ppm 3.38–3.46 (m, 2H, CH₂), 3.54–3.62 (m, 2H, CH₂), 3.82 (s, 3H, OCH₃), 4.78 (bs, 1H, OH), 7.01 (d, *J* = 8.4 Hz, 2H, Ar–H), 7.16 (bs, 1H, NH), 7.31 (t, *J* = 6.0 Hz, 2H, Ar–H), 7.68 (d, *J* = 15.6 Hz, 1H, CH), 7.81–7.89 (m, 5H, Ar–H, CH), 8.01 (d, *J* = 8.4 Hz, 2H, Ar–H), 8.09 (t, *J* = 8.2 Hz, 2H, Ar–H), 9.32 (bs, 1H, NH), 9.55 (bs, 1H, NH). ¹³C-NMR (100 MHz, DMSO-*d*₆) δ ppm 43.0 (CH₂), 55.4 (CH₃), 59.9 (CH₂), 114.4 (CH), 118.8 (CH), 119.7 (CH), 121.4 (CH), 125.3 (Cq), 127.5 (Cq), 128.2 (CH), 129.5 (CH), 130.6 (CH), 130.9 (Cq), 139.3 (Cq), 142.9 (CH), 145.0 (Cq), 161.2 (Cq), 163.9 (Cq), 164.1 (Cq), 165.8 (Cq), 187.3 (Cq). MS (70 eV) *m/z* (%): 516 : 518 [*M*⁺] : [*M* + 2]⁺ (100/50), 486 (57), 473 (50), 356 (52), 236 (39), 161 (20), 121 (17), 77 (20). Anal. calcd C₂₇H₂₅ClN₆O₃: C, 62.73; H, 4.87; N, 16.26; found: C, 62.70; H, 4.90; N, 16.29.

4.2.7.4. (*E*)-1-4-((4-((4-Chlorophenyl)amino)-6-((2-hydroxyethyl)amino)-1,3,5-triazin-2-yl)amino)phenyl)-3-(3,4,5-trimethoxyphenyl)prop-2-en-1-one (**8d**). Yellow solid. 91% yield; mp 242–246 °C. FT-IR (ATR): ν (cm⁻¹) 3564 (N–H), 3290 (O–H), 3098 (=C–H), 1649 (C=O), 1560 γ 1516 (C=N and C=C). ¹H-NMR (400 MHz, DMSO-*d*₆) δ ppm 3.65–3.52 (m, 4H), 3.72 (s, 3H, OCH₃), 3.87 (s, 6H, OCH₃), 4.79 (bs, 1H, OH), 7.16 (bs, 1H, NH), 7.22 (s, 2H, Ar–H), 7.31 (t, *J* = 6.0 Hz, 2H, Ar–H), 7.66 (d, *J* = 15.6 Hz, 1H, CH), 7.93–7.76 (m, 3H, Ar–H), 8.03 (d, *J* = 7.6 Hz, 2H, Ar–H), 8.13 (t, *J* = 8.2 Hz, 2H, Ar–H), 9.32 (bs, 1H, NH), 9.57 (bs, 1H, NH). ¹³C-NMR (100 MHz, DMSO-*d*₆) δ ppm 43.0 (CH₂), 56.2 (CH₃), 59.9 (CH₂), 60.2 (CH₃), 106.4 (CH), 107.1 (CH), 118.8 (CH), 121.5 (CH), 125.3 (Cq), 128.2 (CH), 129.7 (CH), 130.5 (Cq), 130.8 (Cq), 139.2 (Cq), 139.6 (Cq), 143.4 (CH), 152.4 (Cq), 153.2 (Cq), 163.9 (Cq), 164.1 (Cq), 165.8 (Cq), 187.4 (Cq). MS (70 eV) *m/z* (%): 576 : 578 [*M*⁺] : [*M* + 2]⁺ (94/46), 561 (25), 545 (27), 501 (21), 356 (21), 195 (44), 98 (40), 84 (96). Anal. calcd C₂₉H₂₉ClN₆O₅: C, 60.36; H, 5.07; N, 14.56; found: C, 60.40; H, 5.03; N, 14.49.

4.2.7.5. (*E*)-3-(4-Chlorophenyl)-1-4-((4-((4-chlorophenyl)amino)-6-((2-hydroxyethyl)amino)-1,3,5-triazin-2-yl)amino)phenyl)prop-2-en-1-one (**8e**). Yellow solid. 93% yield; mp 200–204 °C. FT-IR (ATR): ν (cm⁻¹) 3400 (N–H), 3279 (O–H), 3117 (=C–H), 1641 (C=O), 1577 γ 1529 (C=N and C=C). ¹H-NMR (400 MHz, DMSO-*d*₆) δ ppm 3.38–3.47 (m, 2H, CH₂), 3.54–3.61 (m, 2H, CH₂), 4.77 (s, 1H, OH), 7.17 (bs, 1H, NH), 7.31 (t, *J* = 7.5 Hz, 2H, Ar–H), 7.51 (d, *J* = 8.4 Hz, 2H, Ar–H), 7.68 (d, *J* = 15.6 Hz, 1H, CH), 7.82–7.89 (m, 2H, Ar–H), 7.92 (d, *J* = 8.4 Hz, 2H, Ar–H), 7.94–8.05 (m, 3H, Ar–H, CH), 8.11 (t, *J* = 8.8 Hz, 2H, Ar–H), 9.41 (bs, 2H, NH). ¹³C-NMR (100 MHz, DMSO-*d*₆) δ ppm 43.0 (CH₂), 59.9 (CH₂), 118.7 (CH), 121.4 (CH), 123.0 (CH), 125.3 (Cq), 128.1 (CH), 128.9 (CH), 129.7 (CH), 130.5 (CH), 133.9 (Cq), 134.8 (Cq), 139.2 (Cq), 141.4 (CH), 143.6 (Cq), 145.3 (Cq), 163.8 (Cq), 164.0 (Cq), 165.8 (Cq), 187.2 (Cq). MS (70 eV) *m/z* (%): 520 : 522 : 524 [*M*⁺] : [*M* + 2]⁺ : [*M* + 4]⁺ (20/14/4), 491 (19), 477 (23), 475 (15), 367 (11), 339 (12), 178 (20), 145 (25), 135 (32). Anal. calcd C₂₆H₂₂Cl₂N₆O₂: C, 59.89; H, 4.25; N, 16.12; found: C, 60.01; H, 4.25; N, 16.16.

4.2.7.6. (*E*)-1-4-((4-((4-Chlorophenyl)amino)-6-((2-hydroxyethyl)amino)-1,3,5-triazin-2-yl)amino)phenyl)-3-(4-fluorophenyl)prop-2-en-1-one (**8f**). Yellow solid. 85% yield; mp 196–200 °C. FT-IR (ATR): ν (cm⁻¹) 3412 (N–H), 3279 (O–H), 3117 (=C–H), 1641 (C=O), 1576 γ

1529 (C=N and C=C). ¹H-NMR (400 MHz, DMSO-*d*₆) δ ppm 3.38–3.52 (m, 2H, CH₂), 3.52–3.64 (m, 2H, CH₂), 4.74 (s, 1H, OH), 7.17 (bs, 1H, NH), 7.26–7.36 (m, 4H, Ar–H), 7.71 (d, *J* = 15.6 Hz, 1H, CH), 7.82–7.88 (m, 2H, Ar–H), 7.88–7.99 (m, 3H, Ar–H, CH), 8.03 (d, *J* = 8.4 Hz, 2H, Ar–H), 8.12 (t, *J* = 8.8 Hz, 2H, Ar–H), 9.33 (bs, 1H, NH), 9.57 (bs, 1H, NH). ¹³C-NMR (100 MHz, DMSO-*d*₆) δ ppm 43.0 (CH₂), 59.9 (CH₂), 115.9 (d, ²*J*_{CF} = 21.8 Hz, (CH)), 118.7 (CH), 121.4 (CH), 122.1 (CH), 125.3 (Cq), 128.2 (CH), 129.7 (CH), 130.6 (Cq), 131.1 (d, ³*J*_{CF} = 8.6 Hz, (CH)), 131.6 (d, ⁴*J*_{CF} = 2.9 Hz, Cq), 139.2 (Cq), 141.7 (CH), 145.2 (Cq), 163.1 (d, ¹*J*_{CF} = 201.6 Hz, Cq), 163.8 (Cq), 164.5 (Cq), 165.7 (Cq), 187.3 (Cq). MS (70 eV) *m/z* (%): 504 : 506 [*M*⁺] : [*M* + 2]⁺ (74/32), 474 (65), 461 (60), 313 (71), 264 (81), 236 (100), 98 (78), 84 (67). Anal. calcd C₂₆H₂₂ClFN₆O₂: C, 61.84; H, 4.39; N, 16.64; found: C, 61.86; H, 4.42; N, 16.70.

4.2.7.7. (*E*)-1-4-((4-((4-Chlorophenyl)amino)-6-((2-hydroxyethyl)amino)-1,3,5-triazin-2-yl)amino)phenyl)-3-(4-(trifluoromethyl)phenyl)prop-2-en-1-one (**8g**). Yellow solid. 83% yield; mp 235–240 °C. FT-IR (ATR): ν (cm⁻¹) 3441 (N–H), 3281 (O–H), 3119 (=C–H), 1643 (C=O), 1574 γ 1528 (C=N and C=C). ¹H-NMR (400 MHz, DMSO-*d*₆) δ ppm 3.38–3.49 (m, 2H, CH₂), 3.53–3.63 (m, 2H, CH₂), 4.74 (s, 1H, OH), 7.18 (bs, 1H, NH), 7.25–7.37 (m, 2H, Ar–H), 7.76 (d, *J* = 16.0 Hz, 1H, CH), 7.81 (d, *J* = 8.0 Hz, 2H, Ar–H), 7.83–7.89 (m, 2H, Ar–H), 7.98–8.19 (m, 7H, Ar–H), 9.33 (bs, 1H, NH), 9.59 (bs, 1H, NH). ¹³C-NMR (100 MHz, DMSO-*d*₆) δ ppm 43.0 (CH₂), 59.8 (CH₂), 118.7 (CH), 121.3 (CH), 124.1 (q, ¹*J*_{CF} = 272.2 Hz, CF₃), 124.9 (CH), 125.3 (Cq), 125.4 (Cq), 125.7 (q, ⁴*J*_{CF} = 3.0 Hz, (CH)), 128.2 (CH), 129.3 (CH), 129.8 (q, ³*J*_{CF} = 18.6 Hz, (CH)), 130.3 (Cq), 138.9 (Cq), 139.2 (Cq), 139.2 (Cq), 140.9 (CH), 145.4 (Cq), 163.9 (q, ²*J*_{CF} = 23.2 Hz, Cq), 165.7 (Cq), 187.2 (Cq). MS (70 eV) *m/z* (%): 554 : 556 [*M*⁺] : [*M* + 2]⁺ (100/37), 535 (12), 524 (93), 511 (93), 452 (15), 199 (9), 127 (12), 98 (9). Anal. calcd C₂₇H₂₂ClF₃N₆O₂: C, 58.44; H, 4.00; N, 15.14; found: C, 58.39; H, 4.09; N, 15.10.

4.2.8. General procedure for the synthesis of 2-((4-((4-(1-(3,5-dichlorophenyl)-5-(aryl)-4,5-dihydro-1H-pyrazol-3-yl)phenyl)amino)-6-morpholino-1,3,5-triazin-2-yl)amino)ethanol (**9a–g**). A mixture of chalcone **7** (1 equiv.) and 3,5-dichlorophenylhydrazine hydrochloride (3 equiv.) in ethanol (2.5 mL) was subjected to reflux for 12 h. The solid formed was filtered and washed with ethanol. No further purification was required.

4.2.8.1. 2-((4-((4-(1-(3,5-Dichlorophenyl)-5-phenyl-4,5-dihydro-1H-pyrazol-3-yl)phenyl)amino)-6-morpholino-1,3,5-triazin-2-yl)amino)ethan-1-ol (**9a**). Yellow solid. 78% yield; mp 279–281 °C. FT-IR (ATR): ν (cm⁻¹) 3416 (N–H), 3202 (O–H), 3090 (=C–H), 1626 γ 1599 (C=N and C=C). ¹H-NMR (400 MHz, DMSO-*d*₆) δ ppm 3.16 (dd, *J* = 17.4, 4.6 Hz, 1H, H-4), 3.38–3.49 (m, 2H, CH₂), 3.52–3.60 (m, 2H, CH₂), 3.64–3.72 (m, 5H, CH₂, OH), 3.74–3.84 (m, 4H, CH₂), 3.94 (dd, *J* = 17.4, 11.8 Hz, 1H, H-4), 5.59 (dd, *J* = 11.8, 4.2 Hz, 1H, H-5), 6.80 (s, 1H, Ar–H), 6.93 (s, 2H, Ar–H), 7.23–7.31 (m, 3H, Ar–H), 7.32–7.40 (m, 2H, Ar–H), 7.63–7.82 (m, 4H, Ar–H), 8.30 (bs, 1H, NH), 10.59 (bs, 1H, NH). ¹³C-NMR (100 MHz, DMSO-*d*₆) δ ppm 43.2 (CH₂), 44.1 (CH₂), 44.3 (CH₂), 59.3 (CH₂), 62.4 (CH), 65.7 (CH₂), 110.8 (CH), 116.8 (Cq), 116.9 (CH), 120.3 (CH), 121.0 (Cq), 125.7 (CH), 126.8 (Cq), 126.9 (CH), 127.8 (CH), 129.2 (CH), 134.4 (Cq), 141.4 (Cq), 145.1 (Cq), 145.7 (Cq), 148.0 (Cq), 149.7 (Cq). MS (70 eV) *m/z* (%): 604 : 606 : 608 [*M*⁺] : [*M* + 2]⁺ : [*M* + 4]⁺ (100/70/15), 588 (4), 574 (9), 527 (8), 310 (10), 287 (8), 252 (8). Anal. calcd C₃₀H₃₀Cl₂N₈O₂: C, 59.51; H, 4.99; N, 18.51; found: C, 60.00; H, 4.89; N, 18.53.



4.2.8.2. 2-((4-((4-(1-(3,5-Dichlorophenyl)-5-(*p*-tolyl)-4,5-dihydro-1H-pyrazol-3-yl)phenyl)amino)-6-morpholino-1,3,5-triazin-2-yl)amino)ethan-1-ol (**9b**). Yellow solid. 83% yield; mp 262–265 °C. FT-IR (ATR): ν (cm⁻¹) 3454 (N–H), 3248 (O–H), 3088 (=C–H), 1626 y 1599 (C=N and C=C). ¹H-NMR (400 MHz, DMSO-*d*₆) δ ppm 2.24 (s, 3H, CH₃), 3.10 (dd, *J* = 17.2, 3.8 Hz, 1H, H-4), 3.38–3.49 (m, 2H, CH₂), 3.50–3.72 (m, 7H, CH₂, OH), 3.82–3.74 (m, 4H, CH₂), 3.89 (dd, *J* = 17.2, 11.6 Hz, 1H, H-4), 5.51 (dd, *J* = 11.6, 3.8 Hz, 1H, H-5), 6.77 (s, 1H, Ar–H), 6.91 (s, 2H, Ar–H), 7.18–7.09 (m, 4H, Ar–H), 7.62–7.80 (m, 4H, Ar–H), 8.36 (bs, 1H, NH), 10.65 (bs, 1H, NH). ¹³C-NMR (100 MHz, DMSO-*d*₆) δ ppm 20.7 (CH₃), 43.1 (CH₂), 43.3 (CH₂), 44.4 (CH₂), 59.1 (CH₂), 62.3 (CH), 65.8 (CH₂), 110.9 (CH), 116.9 (CH), 116.9 (Cq), 120.5 (CH), 121.2 (Cq), 125.8 (CH), 127.0 (CH), 127.3 (Cq), 129.8 (CH), 134.5 (Cq), 137.1 (Cq), 138.5 (Cq), 139.6 (Cq), 145.8 (Cq), 148.8 (Cq), 149.8 (Cq). MS (70 eV) *m/z* (%): 618 : 620 : 622 [M^+] : [$M + 2$]⁺ : [$M + 4$]⁺ (100/68/14), 587 (8), 527 (14), 310 (12), 294 (7), 252 (6), 117 (9), 91 (9). Anal. calcd C₃₁H₃₂Cl₂N₈O₂: C, 60.10; H, 5.21; N, 18.09; found: C, 60.15; H, 5.18; N, 18.10.

4.2.8.3. 2-((4-((4-(1-(3,5-Dichlorophenyl)-5-(4-methoxyphenyl)-4,5-dihydro-1H-pyrazol-3-yl)phenyl)amino)-6-morpholino-1,3,5-triazin-2-yl)amino)ethan-1-ol (**9c**). Yellow solid. 75% yield; mp 275–278 °C. FT-IR (ATR): ν (cm⁻¹) 3327 (N–H), 3252 (O–H), 3094 (=C–H), 1661 y 1582 (C=N and C=C). ¹H-NMR (400 MHz, DMSO-*d*₆) δ ppm 3.12 (dd, *J* = 17.2, 3.7 Hz, 1H, H-4), 3.44 (d, *J* = 18.5 Hz, 2H, CH₂), 3.50–3.60 (m, 2H, CH₂), 3.61–3.74 (m, 7H, CH₂, OCH₃), 3.75–3.82 (m, 4H, CH₂), 3.89 (dd, *J* = 17.2, 11.9 Hz, 1H, H-4), 4.50 (bs, 1H, OH), 5.52 (dd, *J* = 11.9, 3.7 Hz, 1H, H-5), 6.79 (s, 1H, Ar–H), 6.82–6.98 (m, 4H, Ar–H), 7.18 (d, *J* = 8.2 Hz, 2H, Ar–H), 7.65–7.85 (m, 4H, Ar–H), 8.46 (bs, 1H, NH), 10.76 (bs, 1H, NH). ¹³C-NMR (100 MHz, DMSO-*d*₆) δ ppm 43.0 (CH₂), 43.2 (CH₂), 44.4 (CH₂), 55.0 (OCH₃), 59.0 (CH₂), 61.9 (CH), 65.7 (CH₂), 110.8 (CH), 114.5 (CH), 116.8 (CH), 120.3 (CH), 120.4 (Cq), 121.0 (Cq), 126.7 (Cq), 126.9 (CH), 127.0 (CH), 127.2 (Cq), 133.2 (Cq), 134.3 (Cq), 145.7 (Cq), 149.6 (Cq), 149.7 (Cq), 158.7 (Cq). MS (70 eV) *m/z* (%): 634 : 636 : 638 [M^+] : [$M + 2$]⁺ : [$M + 4$]⁺ (100/70/15), 604 (5), 527 (39), 310 (12), 280 (7), 252 (6), 134 (14), 121 (14). Anal. calcd C₃₁H₃₂Cl₂N₈O₃: C, 58.59; H, 5.08; N, 17.63; found: C, 58.62; H, 5.12; N, 17.59.

4.2.8.4. 2-((4-((4-(1-(3,5-Dichlorophenyl)-5-(3,4,5-trimethoxyphenyl)-4,5-dihydro-1H-pyrazol-3-yl)phenyl)amino)-6-morpholino-1,3,5-triazin-2-yl)amino)ethan-1-ol (**9d**). Yellow solid. 80% yield; mp 239–242 °C. FT-IR (ATR): ν (cm⁻¹) 3410 (N–H), 3242 (O–H), 3098 (=C–H), 1659 y 1583 (C=N and C=C). ¹H-NMR (400 MHz, DMSO-*d*₆) δ ppm 3.20 (dd, *J* = 17.7, 6.2 Hz, 1H, H-4), 3.36–3.43 (m, 2H, CH₂), 3.49–3.54 (m, 2H, CH₂), 3.59–3.66 (m, 7H, OCH₃, CH₂), 3.67–3.73 (m, 10H, OCH₃, CH₂), 3.90 (dd, *J* = 17.7, 11.7 Hz, 1H, H-4), 4.67 (s, 1H, OH), 5.39 (dd, *J* = 11.7, 6.2 Hz, 1H, H-5), 6.60 (s, 2H, Ar–H), 6.76–6.89 (m, 2H, Ar–H, NH), 6.96 (s, 2H, Ar–H), 7.68 (t, *J* = 7.2 Hz, 2H, Ar–H), 7.83 (d, *J* = 8.7 Hz, 2H, Ar–H), 9.24 (bs, 1H, NH). ¹³C-NMR (100 MHz, DMSO-*d*₆) δ ppm 42.9 (CH₂), 43.0 (CH₂), 43.3 (CH₂), 56.0 (OCH₃), 59.9 (CH₂), 60.0 (OCH₃), 63.0 (CH), 66.0 (CH₂), 103.0 (CH), 109.7 (Cq), 110.9 (CH), 116.1 (CH), 119.1 (CH), 122.5 (Cq), 126.8 (CH), 131.2 (Cq), 134.4 (Cq), 136.8 (Cq), 137.4 (Cq), 149.0 (Cq), 150.5 (Cq), 153.2 (Cq), 153.4 (Cq), 158.7 (Cq). MS (70 eV) *m/z* (%): 694 : 696 : 698

[M^+] : [$M + 2$]⁺ : [$M + 4$]⁺ (100/72/15), 677 (6), 527 (49), 310 (15), 280 (7), 252 (14), 179 (15), 83 (27). Anal. calcd C₃₃H₃₆Cl₂N₈O₅: C, 56.98; H, 5.22; N, 16.11; found: C, 57.01; H, 5.20; N, 16.15.

4.2.8.5. 2-((4-((4-(5-(4-Chlorophenyl)-1-(3,5-dichlorophenyl)-4,5-dihydro-1H-pyrazol-3-yl)phenyl)amino)-6-morpholino-1,3,5-triazin-2-yl)amino)ethan-1-ol (**9e**). Yellow solid. 91% yield; mp 230–234 °C. FT-IR (ATR): ν (cm⁻¹) 3520 (N–H), 3273 (O–H), 3105 (=C–H), 1653 y 1582 (C=N and C=C). ¹H-NMR (400 MHz, DMSO-*d*₆) δ ppm 3.15 (dd, *J* = 17.7, 4.4 Hz, 1H, H-4), 3.44 (d, *J* = 18.5 Hz, 2H, CH₂), 3.50–3.60 (m, 2H, CH₂), 3.62–3.74 (m, 4H, CH₂), 3.74–3.83 (m, 5H, CH₂, OH), 3.92 (dd, *J* = 17.7, 11.7 Hz, 1H, H-4), 5.63 (dd, *J* = 11.7, 4.4 Hz, 1H, H-5), 6.80 (s, 1H, Ar–H), 6.92 (s, 2H, Ar–H), 7.27 (d, *J* = 8.4 Hz, 2H, Ar–H), 7.42 (d, *J* = 8.4 Hz, 2H, Ar–H), 7.63–7.81 (m, 4H, Ar–H), 8.48 (bs, 1H, NH), 10.77 (bs, 1H, NH). ¹³C-NMR (100 MHz, DMSO-*d*₆) δ ppm 43.0 (CH₂), 43.3 (CH₂), 44.4 (CH₂), 59.0 (CH₂), 61.6 (CH), 65.7 (CH₂), 110.9 (CH), 117.1 (CH), 117.1 (Cq), 120.4 (Cq), 120.4 (CH), 121.0 (Cq), 124.0 (Cq), 127.0 (CH), 127.8 (CH), 129.2 (CH), 132.3 (Cq), 134.5 (Cq), 140.3 (Cq), 145.5 (Cq), 149.5 (Cq), 149.9 (Cq). MS (70 eV) *m/z* (%): 638 : 640 : 642 : 644 [M^+] : [$M + 2$]⁺ : [$M + 4$]⁺ : [$M + 6$]⁺ (49/41/14/3), 607 (6), 527 (4), 310 (10), 239 (7), 185 (7), 123 (26), 97 (40). Anal. calcd C₃₀H₂₉Cl₃N₈O₂: C, 56.30; H, 4.57; N, 17.51; found: C, 56.20; H, 4.60; N, 17.48.

4.2.8.6. 2-((4-((4-(1-(3,5-Dichlorophenyl)-5-(4-fluorophenyl)-4,5-dihydro-1H-pyrazol-3-yl)phenyl)amino)-6-morpholino-1,3,5-triazin-2-yl)amino)ethan-1-ol (**9f**). Yellow solid. 86% yield; mp 249–252 °C. FT-IR (ATR): ν (cm⁻¹) 3535 (N–H), 3244 (O–H), 3113 (=C–H), 1653 y 1587 (C=N and C=C). ¹H-NMR (400 MHz, DMSO-*d*₆) δ ppm 3.16 (dd, *J* = 17.4, 3.5 Hz, 1H, H-4), 3.44 (d, *J* = 18.4 Hz, 2H, CH₂), 3.51–3.61 (m, 2H, CH₂), 3.63–3.72 (m, 4H, CH₂), 3.75–3.84 (m, 4H, CH₂), 4.06 (bs, 1H, OH), 3.92 (dd, *J* = 17.4, 12.1 Hz, 1H, H-4), 5.62 (dd, *J* = 12.1, 3.5 Hz, 1H, H-5), 6.80 (s, 1H, Ar–H), 6.93 (s, 2H, Ar–H), 7.18 (t, *J* = 8.2 Hz, 2H, Ar–H), 7.25–7.35 (m, 2H, Ar–H), 7.70 (t, *J* = 11.2 Hz, 2H, Ar–H), 7.78 (d, *J* = 8.4 Hz, 2H, Ar–H), 8.50 (bs, 1H, NH), 10.80 (bs, 1H, NH). ¹³C-NMR (100 MHz, DMSO-*d*₆) δ ppm 43.1 (CH₂), 43.3 (CH₂), 44.4 (CH₂), 59.0 (CH₂), 61.6 (CH), 65.7 (CH₂), 110.9 (CH), 116.0 (d, ²*J*_{CF} = 21.5 Hz, (CH)), 117.0 (CH), 117.1 (Cq), 120.4 (CH), 120.9 (Cq), 127.0 (CH), 127.9 (d, ³*J*_{CF} = 8.3 Hz, (CH)), 134.4 (Cq), 137.5 (d, ⁴*J*_{CF} = 3.2 Hz, Cq), 138.4 (Cq), 145.6 (Cq), 149.3 (Cq), 149.7 (Cq), 149.8 (Cq), 161.5 (d, ¹*J*_{C-F} = 244.0 Hz, Cq). MS (70 eV) *m/z* (%): 622 : 624 : 626 [M^+] : [$M + 2$]⁺ : [$M + 4$]⁺ (100/71/15), 592 (11), 527 (10), 310 (16), 266 (11), 124.69 (33). Anal. calcd C₃₀H₂₉Cl₂FN₈O₂: C, 57.79; H, 4.69; N, 17.97; found: C, 57.90; H, 4.72; N, 18.00.

4.2.8.7. 2-((4-((4-(1-(3,5-Dichlorophenyl)-5-(4-(trifluoromethyl)phenyl)-4,5-dihydro-1H-pyrazol-3-yl)phenyl)amino)-6-morpholino-1,3,5-triazin-2-yl)amino)ethan-1-ol (**9g**). Yellow solid. 84% yield; mp 258–263 °C. FT-IR (ATR): ν (cm⁻¹) 3445 (N–H), 3242 (O–H), 3105 (=C–H), 1653 y 1584 (C=N and C=C). ¹H-NMR (400 MHz, DMSO-*d*₆) δ ppm 3.21 (dd, *J* = 17.8, 4.2 Hz, 1H, H-4), 3.44 (d, *J* = 16.4 Hz, 2H, CH₂), 3.50–3.60 (m, 2H, CH₂), 3.62–3.73 (m, 5H, CH₂, OH), 3.74–3.85 (m, 4H, CH₂), 3.96 (dd, *J* = 17.8, 11.8 Hz, 1H, H-4), 5.75 (dd, *J* = 11.8, 4.2 Hz, 1H, H-5), 6.82 (s, 1H, Ar–H), 6.93 (s, 2H, Ar–H), 7.48 (d, *J* = 8.4 Hz, 2H, Ar–H), 7.62–7.86 (m, 6H, Ar–H), 8.40 (bs, 1H, NH), 10.72 (bs, 1H, NH). ¹³C-NMR (100 MHz, DMSO-*d*₆) δ ppm 42.9 (CH₂), 44.1 (CH₂), 44.4 (CH₂), 59.0 (CH₂), 61.7 (CH), 65.8 (CH₂), 110.8 (CH), 110.9 (Cq), 113.0 (Cq), 114.1 (Cq), 117.2 (CH), 118.2 (Cq), 120.3 (Cq), 120.4 (Cq), 120.9 (CH), 121.0 (q, ¹*J*_{CF}



= 244.51 Hz, CF₃), 125.5 (Cq), 126.2 (d, ³J_{CF} = 5.7 Hz, (CH)), 126.8 (CH), 127.0 (d, ⁴J_{CF} = 1.2 Hz, (CH)), 134.6 (Cq), 145.8 (d, ²J_{CF} = 46.76 Hz, Cq), 150.0 (Cq). MS (70 eV) *m/z* (%): 672 : 674 : 676 [M⁺] : [M + 2]⁺ : [M + 4]⁺ (100/66/13), 642 (12), 515 (7), 310 (14), 252 (8), 124 (25), 69 (32). Anal. calcd C₃₁H₂₉Cl₂F₃N₈O₂: C, 55.28; H, 4.34; N, 16.64; found: C, 55.32; H, 4.29; N, 16.58.

4.2.9. General procedure for the synthesis of 2-((4-((4-chlorophenyl)amino)-6-((4-(1-(3,5-dichlorophenyl)-5-(aryl)-4,5-dihydro-1H-pyrazol-3-yl)phenyl)amino)-1,3,5-triazin-2-yl)amino)ethanol (10a-g). A mixture of chalcone 8 (1 equiv.) and 3,5-dichlorophenylhydrazine hydrochloride (3 equiv.) in ethanol (2.5 mL) was subjected to reflux for 12 h. The solid formed was filtered and washed with ethanol. No further purification was required.

4.2.9.1. 2-((4-((4-Chlorophenyl)amino)-6-((4-(1-(3,5-dichlorophenyl)-5-phenyl-4,5-dihydro-1H-pyrazol-3-yl)phenyl)amino)-1,3,5-triazin-2-yl)amino)ethanol-1-ol (10a). Yellow solid. 84% yield; mp 222–224 °C. FT-IR (ATR): ν (cm⁻¹) 3419 (N-H), 3319 (O-H), 3113 (=C-H), 1622 y 1583 (C=N and C=C). ¹H-NMR (400 MHz, DMSO-*d*₆) δ ppm 3.18 (dd, *J* = 17.5, 4.6 Hz, 1H, H-4), 3.32–3.49 (m, 2H, CH₂), 3.57–3.62 (m, 2H, CH₂), 3.75–4.12 (m, 2H, H-4, OH), 5.58 (dd, *J* = 11.9, 4.6 Hz, 1H, H-5), 6.79 (s, 1H, Ar-H), 6.93 (s, 2H, Ar-H), 7.24–7.31 (m, 3H, Ar-H), 7.33–7.44 (m, 4H, Ar-H), 7.68–7.83 (m, 6H, Ar-H), 8.50 (bs, 1H, NH), 10.43 (bs, 1H, NH), 10.65 (bs, 1H, NH). ¹³C-NMR (100 MHz, DMSO-*d*₆) δ ppm 43.2 (CH₂), 43.4 (CH₂), 59.2 (CH₂), 62.5 (CH), 110.8 (CH), 116.9 (CH), 120.7 (CH), 121.2 (CH), 122.7 (Cq), 123.2 (Cq), 123.3 (Cq), 125.8 (CH), 126.6 (Cq), 126.7 (CH), 127.0 (Cq), 127.8 (CH), 128.6 (CH), 129.2 (CH), 134.4 (Cq), 136.8 (Cq), 137.2 (Cq), 141.4 (Cq), 145.8 (Cq), 149.8 (Cq). MS (70 eV) *m/z* (%): 644 : 646 : 648 : 650 [M⁺] : [M + 2]⁺ : [M + 4]⁺ : [M + 6]⁺ (95/100/38/5), 628 (49), 567 (12), 350 (17), 221 (19), 178 (17), 124 (24), 91 (30). Anal. calcd C₃₂H₂₇Cl₃N₈O: C, 59.50; H, 4.21; N, 17.35; found: C, 59.48; H, 4.27; N, 17.40.

4.2.9.2. 2-((4-((4-Chlorophenyl)amino)-6-((4-(1-(3,5-dichlorophenyl)-5-(*p*-tolyl)-4,5-dihydro-1H-pyrazol-3-yl)phenyl)amino)-1,3,5-triazin-2-yl)amino)ethanol-1-ol (10b). Yellow solid. 90% yield; mp 277–279 °C. FT-IR (ATR): ν (cm⁻¹) 3311 (N-H), 3252 (O-H), 3190 (=C-H), 1629 y 1583 (C=N and C=C). ¹H-NMR (400 MHz, DMSO-*d*₆) δ ppm 2.25 (s, 3H, CH₃), 3.14 (dd, *J* = 17.1, 4.4 Hz, 1H, H-4), 3.40–3.50 (m, 2H, CH₂), 3.56–3.62 (m, 2H, CH₂), 3.85–4.00 (m, 2H, H-4, OH), 5.53 (dd, *J* = 12.1, 4.4 Hz, 1H, H-5), 6.79 (s, 1H, Ar-H), 6.93 (d, *J* = 1.6 Hz, 2H, Ar-H), 7.13–7.17 (m, 4H, Ar-H), 7.35–7.45 (m, 2H, Ar-H), 7.67–7.83 (m, 6H, Ar-H), 8.47 (bs, 1H, NH), 10.41 (bs, 1H, NH), 10.62 (bs, 1H, NH). ¹³C-NMR (100 MHz, DMSO-*d*₆) δ ppm 20.7 (CH₃), 43.2 (CH₂), 43.4 (CH₂), 59.2 (CH₂), 62.3 (CH), 110.8 (CH), 116.8 (CH), 120.0 (Cq), 120.8 (CH), 122.7 (Cq), 123.2 (CH), 125.7 (CH), 125.9 (Cq), 126.7 (CH), 127.1 (Cq), 127.6 (Cq), 128.5 (CH), 128.6 (Cq), 129.7 (CH), 134.4 (Cq), 134.5 (Cq), 137.0 (Cq), 138.5 (Cq), 145.8 (Cq), 149.8 (Cq). MS (70 eV) *m/z* (%): 658 : 660 : 662 : 664 [M⁺] : [M + 2]⁺ : [M + 4]⁺ : [M + 6]⁺ (100/98/37/5), 642 (23), 557 (36), 350 (31), 178 (27), 117 (33), 91 (34). Anal. calcd C₃₃H₂₉Cl₃N₈O: C, 60.05; H, 4.43; N, 16.98; found: C, 59.98; H, 4.40; N, 17.01.

4.2.9.3. 2-((4-((4-Chlorophenyl)amino)-6-((4-(1-(3,5-dichlorophenyl)-5-(4-methoxyphenyl)-4,5-dihydro-1H-pyrazol-3-yl)phenyl)amino)-1,3,5-triazin-2-yl)amino)ethanol-1-ol (10c). Yellow solid. 95% yield; mp 276–279 °C. FT-IR (ATR): ν (cm⁻¹) 3308 (N-H), 3246 (O-

H), 3188 (=C-H), 1634 y 1585 (C=N and C=C). ¹H-NMR (400 MHz, DMSO-*d*₆) δ ppm 3.14 (dd, *J* = 17.0, 4.3 Hz, 1H, H-4), 3.42–3.50 (m, 2H, CH₂), 3.55–3.63 (m, 2H, CH₂), 3.71 (s, 3H, OCH₃), 3.76–3.97 (m, 2H, H-4, OH), 5.52 (dd, *J* = 11.6, 4.3 Hz, 1H, H-5), 6.78 (s, 1H, Ar-H), 6.86–6.98 (m, 4H, Ar-H), 7.19 (d, *J* = 8.4, 2H, Ar-H), 7.36–7.44 (m, 2H, Ar-H), 7.65–7.85 (m, 6H, Ar-H), 8.59 (bs, 1H, NH), 10.50 (bs, 1H, NH), 10.76 (bs, 1H, NH). ¹³C-NMR (100 MHz, DMSO-*d*₆) δ ppm 43.2 (CH₂), 43.4 (CH₂), 55.1 (OCH₃), 59.2 (CH₂), 62.0 (CH), 110.9 (CH), 114.5 (CH), 116.8 (CH), 120.8 (CH), 121.3 (Cq), 122.7 (Cq), 123.3 (CH), 126.7 (CH), 126.8 (Cq), 127.1 (CH), 128.5 (Cq), 128.6 (CH), 133.3 (Cq), 134.4 (Cq), 136.6 (CH), 142.1 (Cq), 145.8 (Cq), 149.8 (Cq), 152.2 (Cq), 158.7 (Cq). MS (70 eV) *m/z* (%): 674 : 676 : 678 : 680 [M⁺] : [M + 2]⁺ : [M + 4]⁺ : [M + 6]⁺ (30/29/11/2), 658 (9), 640 (8), 567 (13), 350 (12), 124 (25), 84 (100). Anal. calcd C₃₃H₂₉Cl₃N₈O₂: C, 58.63; H, 4.32; N, 16.58; found: C, 58.66; H, 4.32; N, 16.60.

4.2.9.4. 2-((4-((4-Chlorophenyl)amino)-6-((4-(1-(3,5-dichlorophenyl)-5-(3,4,5-trimethoxyphenyl)-4,5-dihydro-1H-pyrazol-3-yl)phenyl)amino)-1,3,5-triazin-2-yl)amino)ethanol-1-ol (10d). Yellow solid. 86% yield; mp 226–229 °C. FT-IR (ATR): ν (cm⁻¹) 3500 (N-H), 3192 (O-H), 3074 (=C-H), 1636 y 1583 (C=N and C=C). ¹H-NMR (400 MHz, DMSO-*d*₆) δ ppm 3.24 (dd, *J* = 17.4, 5.8 Hz, 1H, H-4), 3.40–3.50 (m, 2H, CH₂), 3.56–3.62 (m, 2H, CH₂), 3.64 (s, 3H, OCH₃), 3.71 (s, 6H, OCH₃), 3.79–3.99 (m, 2H, H-4, OH), 5.43 (dd, *J* = 12.2, 5.8 Hz, 1H, H-5), 6.62 (s, 2H, Ar-H), 6.83 (s, 1H, Ar-H), 6.97 (s, 2H, Ar-H), 7.40 (d, *J* = 6.8 Hz, 2H, Ar-H), 7.68–7.86 (m, 6H, Ar-H), 8.53 (bs, 1H, NH), 10.46 (bs, 1H, NH), 10.68 (s, 1H, NH). ¹³C-NMR (100 MHz, DMSO-*d*₆) δ ppm 43.3 (CH₂), 43.4 (CH₂), 56.0 (OCH₃), 59.2 (CH₂), 60.0 (OCH₃), 63.2 (CH), 103.1 (CH), 111.0 (CH), 117.1 (CH), 120.7 (CH), 120.8 (Cq), 121.2 (Cq), 122.7 (Cq), 123.1 (CH), 123.3 (Cq), 126.7 (Cq), 126.8 (CH), 126.9 (Cq), 128.6 (CH), 134.4 (Cq), 136.8 (Cq), 137.3 (Cq), 139.1 (Cq), 146.2 (Cq), 150.1 (Cq), 153.4 (Cq). MS (70 eV) *m/z* (%): 734 : 736 : 738 : 740 [M⁺] : [M + 2]⁺ : [M + 4]⁺ : [M + 6]⁺ (18/15/6/1), 656 (18), 567 (9), 363 (12), 221 (18), 152 (15), 118 (18). Anal. calcd C₃₅H₃₃Cl₃N₈O₄: C, 57.11; H, 4.52; N, 15.22; found: C, 57.15; H, 4.55; N, 15.32.

4.2.9.5. 2-((4-((4-(5-(4-Chlorophenyl)-1-(3,5-dichlorophenyl)-4,5-dihydro-1H-pyrazol-3-yl)phenyl)amino)-6-((4-chlorophenyl)amino)-1,3,5-triazin-2-yl)amino)ethanol-1-ol (10e). Yellow solid. 95% yield; mp 277–279 °C. FT-IR (ATR): ν (cm⁻¹) 3309 (N-H), 3200 (O-H), 3192 (=C-H), 1632 y 1583 (C=N and C=C). ¹H-NMR (400 MHz, DMSO-*d*₆) δ ppm 3.18 (dd, *J* = 16.5, 4.0 Hz, 1H, H-4), 3.41–3.51 (m, 2H, CH₂), 3.57–3.63 (m, 2H, CH₂), 3.74–4.07 (m, 2H, H-4, OH), 5.63 (dd, *J* = 12.5, 4.0 Hz, 1H, H-5), 6.81 (s, 1H, Ar-H), 6.92 (s, 2H, Ar-H), 7.29 (d, *J* = 8.4 Hz, 2H, Ar-H), 7.36–7.45 (m, 4H, Ar-H), 7.66–7.86 (m, 6H, Ar-H), 8.54 (bs, 1H, NH), 10.46 (bs, 1H, NH), 10.69 (bs, 1H, NH). ¹³C-NMR (100 MHz, DMSO-*d*₆) δ ppm 43.0 (CH₂), 43.4 (CH₂), 59.2 (CH₂), 61.7 (CH), 110.9 (CH), 117.1 (CH), 120.7 (CH), 121.2 (Cq), 121.3 (Cq), 122.7 (Cq), 123.1 (CH), 123.6 (Cq), 125.9 (Cq), 126.8 (CH), 126.9 (Cq), 127.8 (CH), 128.6 (CH), 128.9 (Cq), 129.2 (CH), 132.3 (Cq), 134.5 (Cq), 140.4 (Cq), 145.6 (Cq), 149.9 (Cq). MS (70 eV) *m/z* (%): 678 : 680 : 682 : 684 : 686 [M⁺] : [M + 2]⁺ : [M + 4]⁺ : [M + 6]⁺ : [M + 8]⁺ (70/89/47/11/1), 662 (25), 555 (18), 417 (20), 350 (25), 262 (31), 221 (27), 118 (40). Anal. calcd C₃₂H₂₆Cl₄N₈O: C, 56.49; H, 3.85; N, 16.47; found: C, 56.52; H, 3.87; N, 16.50.



4.2.9.6. 2-((4-((4-Chlorophenyl)amino)-6-((4-(1-(3,5-dichlorophenyl)-5-(4-fluorophenyl)-4,5-dihydro-1H-pyrazol-3-yl)phenyl)amino)-1,3,5-triazin-2-yl)amino)ethan-1-ol (**10f**). Yellow solid. 77% yield; mp 208–211 °C. FT-IR (ATR): ν (cm⁻¹) 3319 (N–H), 3253 (O–H), 3095 (=C–H), 1620 y 1585 (C=N and C=C). ¹H-NMR (400 MHz, DMSO-*d*₆) δ ppm 3.18 (dd, *J* = 16.8, 4.8 Hz, 1H, H-4), 3.40–3.50 (m, 2H, CH₂), 3.56–3.62 (m, 2H, CH₂), 3.86–4.01 (m, 2H, H-4, OH), 5.62 (dd, *J* = 12.3, 4.8 Hz, 1H, H-5), 6.81 (s, 1H, Ar–H), 6.93 (d, *J* = 1.3 Hz, 2H, Ar–H), 7.19 (t, *J* = 8.6 Hz, 2H, Ar–H), 7.28–7.35 (m, 2H, Ar–H), 7.36–7.44 (m, 2H, Ar–H), 7.66–7.86 (m, 6H, Ar–H), 8.50 (bs, 1H, NH), 10.43 (bs, 1H, NH), 10.63 (bs, 1H, NH). ¹³C-NMR (100 MHz, DMSO-*d*₆) δ ppm 43.1 (CH₂), 43.4 (CH₂), 59.2 (CH₂), 61.7 (CH), 110.9 (CH), 116.0 (d, ²*J*_{CF} = 21.5 Hz, (CH)), 117.0 (CH), 120.7 (CH), 120.8 (Cq), 121.3 (Cq), 122.3 (Cq), 122.8 (Cq), 123.2 (CH), 123.5 (Cq), 126.8 (CH), 126.9 (Cq), 127.9 (d, ³*J*_{CF} = 7.8 Hz, (CH)), 128.5 (CH), 128.6 (Cq), 134.4 (Cq), 137.6 (d, ⁴*J*_{CF} = 2.5 Hz, Cq), 145.6 (Cq), 149.8 (Cq), 161.5 (d, ¹*J*_{C–F} = 243.7 Hz, Cq). MS (70 eV) *m/z* (%): 662 : 664 : 666 : 668 [*M*⁺] : [*M* + 2]⁺ : [*M* + 4]⁺ : [*M* + 6]⁺ (65/51/17/3), 644 (25), 557 (9), 350 (13), 279 (13), 262 (17), 221 (27), 124 (25). Anal. calcd C₃₂H₂₆Cl₃FN₈O: C, 57.89; H, 3.95; 2.86; N, 16.88; found: C, 57.90; H, 4.00; N, 16.74.

4.2.9.7. 2-((4-((4-Chlorophenyl)amino)-6-((4-(1-(3,5-dichlorophenyl)-5-(4-(trifluoromethyl)phenyl)-4,5-dihydro-1H-pyrazol-3-yl)phenyl)amino)-1,3,5-triazin-2-yl)amino)ethan-1-ol (**10g**). Yellow solid. 83% yield; mp 274–277 °C. FT-IR (ATR): ν (cm⁻¹) 3310 (N–H), 3292 (O–H), 3190 (=C–H), 1632 y 1585 (C=N and C=C). ¹H-NMR (400 MHz, DMSO-*d*₆) δ ppm 3.17–3.28 (m, 1H, H-4), 3.41–2.51 (m, 2H, CH₂), 3.56–6.63 (m, 2H, CH₂), 3.98 (dd, *J* = 16.6, 12.5 Hz, 1H, H-4), 4.23 (bs, 1H, OH), 5.74 (dd, *J* = 12.5, 4.8 Hz, 1H, H-5), 6.83 (s, 1H, Ar–H), 6.94 (s, 2H, Ar–H), 7.35–7.45 (m, 2H, Ar–H), 7.50 (d, *J* = 8.0 Hz, 2H, Ar–H), 7.68–7.84 (m, 8H, Ar–H), 8.48 (bs, 1H, NH), 10.42 (bs, 1H, NH), 10.61 (bs, 1H, NH). ¹³C-NMR (100 MHz, DMSO-*d*₆) δ ppm 42.9 (CH₂), 43.3 (CH₂), 59.2 (CH₂), 61.8 (CH), 110.8 (CH), 117.2 (CH), 120.5 (Cq), 120.7 (CH), 121.3 (CH), 123.1 (CH), 123.4 (Cq), 124.1 (q, ¹*J*_{CF} = 272.2 Hz, CF₃), 126.2 (Cq), 126.5 (d, ⁴*J*_{CF} = 5.86 Hz, (CH)), 126.8 (d, ³*J*_{CF} = 7.00 Hz, (CH)), 127.6 (Cq), 127.9 (Cq), 128.2 (Cq), 128.6 (CH), 134.5 (Cq), 136.8 (Cq), 137.1 (Cq), 145.8 (d, ²*J*_{CF} = 46.58 Hz, Cq), 148.2 (Cq), 149.9 (Cq). MS (70 eV) *m/z* (%): 712 : 714 : 716 : 718 [*M*⁺] : [*M* + 2]⁺ : [*M* + 4]⁺ : [*M* + 6]⁺ (100/94/35/5), 696 (11), 682 (12), 557 (10), 350 (23), 279 (19), 178 (20), 124 (29). Anal. calcd C₃₃H₂₆Cl₃F₃N₈O: C, 55.52; H, 3.67; N, 15.69; found: C, 55.50; H, 3.69; N, 15.74.

4.3. Anticancer activity

The human cancer cell lines of the cancer screening panel were grown in an RPMI-1640 medium containing 5% fetal bovine serum and 2 mM L-glutamine. For a typical screening experiment, cells were inoculated into 96-well microtiter plates. After cell inoculation, the microtiter plates were incubated at 37 °C, 5% CO₂, 95% air, and 100% relative humidity for 24 h prior to the addition of the tested compounds. After 24 h, two plates of each cell line were fixed *in situ* with TCA, to represent a measurement of the cell population for each cell line at the time of sample addition (*T*_z). The samples were solubilized in dimethyl sulfoxide (DMSO) at 400-fold the desired final maximum test concentration and stored frozen prior to use. At

the time of compound addition, an aliquot of frozen concentrate was thawed and diluted to twice the desired final maximum test concentration with complete medium containing 50 µg mL⁻¹ gentamicin. An additional four 10-fold or 1/2 log serial dilutions were made to provide a total of five drug concentrations plus the control. Aliquots of 100 µL of these different sample dilutions were added to the appropriate microtiter wells already containing 100 µL of medium, resulting in the required final sample concentrations. After the tested compounds were added, the plates were incubated for an additional 48 h at 37 °C, 5% CO₂, 95% air, and 100% relative humidity. For adherent cells, the assay was terminated by the addition of cold TCA. Cells were fixed *in situ* by the gentle addition of 50 µL of cold 50% (w/v) TCA (final concentration, 10% TCA) and incubated for 60 min at 4 °C. The supernatant was discarded, and plates were washed five times with tap water and air dried. Sulforhodamine B (SRB) solution (100 µL) at 0.4% (w/v) in 1% acetic acid was added to each well, and plates were incubated for 10 min at room temperature. After staining, unbound dye was removed by washing five times with 1% acetic acid and the plates were air dried. Bound stain was subsequently solubilized with 10 mM trizma base, and the absorbance was read on an automated plate reader at a wavelength of 515 nm. Using the seven absorbance measurements [time zero (*T*_z), control growth in the absence of drug, and test growth in the presence of drug at the five concentration levels (*T*_i)], the percentage growth was calculated at each of the drug concentrations levels. Percentage growth inhibition was calculated as $[(T_i - T_z)/(C - T_z)] \times 100$ for concentrations for which *T*_i > *T*_z, and $[(T_i - T_z)/T_z] \times 100$ for concentrations for which *T*_i < *T*_z. Two dose-response parameters were calculated for each compound. Growth inhibition of 50% (GI₅₀) was calculated from $[(T_i - T_z)/(C - T_z)] \times 100 = 50$, which is the drug concentration resulting in a 50% lower net protein increase in the treated cells (measured by SRB staining) as compared to the net protein increase seen in the control cells and the LC₅₀ (concentration of drug resulting in a 50% reduction in the measured protein at the end of the drug treatment as compared to that at the beginning), indicating a net loss of cells; calculated from $[(T_i - T_z)/T_z] \times 100 = -50$. Values were calculated for each of these two parameters if the level of activity is reached; however, if the effect was not reached or was exceeded, the value for that parameter was expressed as greater or less than the maximum or minimum concentration tested.³⁸

4.4. Molecular modeling

4.4.1. Ligand based studies. The synthesized molecules were submitted to Biotarget Finder module, available in the web-server <http://www.drudit.com>.³⁴ The tool allows to predict the binding affinity of candidate molecules *versus* a large database of biological targets. The templates of the biological targets are built by using a set of known modulators implemented in the system. The synthesized compounds are submitted to Biological Predictor module by using the default parameters, and the output results are obtained as DAS (Drudit Affinity Score) for



each structure (see user manual available at <http://www.drudit.com> for further details).

4.4.2. Structure based studies

4.4.2.1. Ligand preparation. The default setting of the LigPrep tool implemented in Schrödinger's software (version 2017-1) has been used to prepare the ligands for docking.³⁹ All possible tautomers and combination of stereoisomers have been generated for pH 7.0 \pm 0.4, using the Epik ionization method.⁴⁰ Energy minimization is subsequently done using the integrated OPLS 2005 force field.⁴¹

4.4.2.2. Protein preparation. The high-resolution (2.79 Å) X-ray structure of Human thymidylate synthase complexed with dUMP and raltitrexed (PDB ID: 5X5Q)³⁵ is downloaded from the Protein Databank.³⁶

The receptor grid preparation has been carried out with substrate dUMP and without water molecules, to elucidate the role of dUMP for the binding, by assigning the original ligand (raltitrexed) as the centroid of the grid box. Protein Preparation Wizard of Schrödinger software that was employed using the default settings.⁴² Bond orders have been assigned and hydrogen atoms added as well as protonation of the heteroatom states using Epik-tool (with the pH set at biologically relevant values, *i.e.* at 7.0 \pm 0.4). The H-bond network has been then optimized. The structure is finally subjected to a restrained energy minimization step (rmsd of the atom displacement for terminating the minimization was 0.3 Å), using the Optimized Potentials for Liquid Simulations (OPLS) 2005 force field.⁴¹

4.4.3. Docking validation. Molecular Docking is performed by Glide program.^{43–45} The generated 3D conformers of the ligands are docked into the receptor model using the Extra Precision (XP) mode as the scoring function. A total of 5 poses per ligand conformer are included in the post-docking minimization step, and a maximum of 2 docking poses are generated for each ligand conformer. The proposed docking procedure was validated by the re-dock of the crystallized raltitrexed within the receptor-binding pocket. The results obtained was in good agreement of the experimental poses, showing a RMSD of 0.79.

4.4.4. Induced fit docking. Induced fit docking simulation is performed using the IFD^{46,47} application as available in the Schrödinger software suite,⁴⁸ which is demonstrated to be an accurate and robust method to account for both ligand and receptor flexibility.⁴⁹ The IFD protocol is carried out as follows:^{50,51} the ligands are docked into the rigid receptor models with scaled-down van der Waals (vdW) radii. The Glide Extra Precision (XP) mode is used for the docking, and 20 ligand poses are retained for protein structural refinements. The docking boxes are defined to include all amino acid residues within the dimensions of 25 Å \times 25 Å \times 25 Å from the center of the original ligands; the induced-fit protein–ligand complexes are generated using the Prime software.⁵² The 20 structures from the previous step are submitted to side chain and backbone refinements. All residues with at least one atom located within 5.0 Å of each corresponding ligand pose are included in the refinement by Prime. All the poses generated are then hierarchically classified, refined and further minimized into the active site grid before being finally scored using the proprietary

GlideScore function, defined as: $Gscore = 0.065 \times vdW + 030 \times Coul + Lipo + Hbond + Metal + BuryP + RotB + Site$, where: vdW is the van der Waals energy term, Coul is the Coulomb energy, Lipo is a lipophilic contact term which rewards favorable hydrophobic interactions, Hbond is an H-bonding term, metal is a metal-binding term (where applicable), BuryP is a penalty term applied to buried polar groups, RotB is a penalty for freezing rotatable bonds and site is a term used to describe favourable polar interactions in the active site.

Finally, IFD score (IFD score = 1.0 Glide Gscore + 0.05 prime energy), which accounts for both protein–ligand interaction energy and total energy of the system, is calculated and used to rank the IFD poses. The more negative is the IFDscore, the more favorable is the binding.

Conflicts of interest

There are no conflicts to declare.

Acknowledgements

The authors thank The Developmental Therapeutics Program (DTP) of the National Cancer Institute of the United States for performing the anticancer screening of the compounds. This work was financially supported by COLCIENCIAS and Universidad del Valle, Colombia.

References

- 1 P. Martins, J. Jesus, S. Santos, L. Raposo, C. Roma, P. Baptista and A. Fernandes, *Molecules*, 2015, **20**, 16852–16891.
- 2 G. Facchetti and I. Rimoldi, *Bioorg. Med. Chem. Lett.*, 2019, **29**, 1257–1263.
- 3 R. Kurukulasuriya, J. Rohde, B. Szczepankiewicz, F. Basha, C. Lai, H. Jae, M. Winn, K. Stewart, K. Longenecker, T. Lubben, S. Ballaron, H. Sham and T. von Geldern, *Bioorg. Med. Chem. Lett.*, 2006, **16**, 6226–6230.
- 4 R. Roskoski, *Pharmacol. Res.*, 2019, **144**, 19–50.
- 5 S. Cascioferro, B. Parrino, V. Spanò, A. Carbone, A. Montalbano, P. Barraja, P. Diana and G. Cirrincione, *Eur. J. Med. Chem.*, 2017, **142**, 523–549.
- 6 G. Riham, K. Manal, E. Dina and E. Ahmed, *Bioorg. Chem.*, 2020, **99**, 103780.
- 7 S. Ranjbaria, M. Behzadib, S. Sepehr, M. Dadkhah, A. Jarrahpoura, M. Mohkame, Y. Ghasemib, A. Reza, S. Kianpourb, Z. Atioğlu, N. Özdemiri, M. Akkurtj, M. Nabavizadeha and E. Turos, *Bioorg. Med. Chem.*, 2020, **28**, 115408.
- 8 S. Kuthyala, M. Hanumanthappa, S. Madan Kumar, S. Sheik, N. Gundibasappa Karikannar and A. Prabhu, *J. Mol. Struct.*, 2019, **1197**, 65–72.
- 9 H. Kothayer, S. Spencer, K. Tripathi, A. Westwell and K. Palle, *Bioorg. Med. Chem. Lett.*, 2016, **26**, 2030–2034.
- 10 Z. Nie, C. Perretta, P. Erickson, S. Margosiak, J. Lu, A. Averill, R. Almassy and S. Chu, *Bioorg. Med. Chem. Lett.*, 2008, **18**, 619–623.



- 11 B. Zhang, Q. Zhang, Z. Xiao, X. Sun, Z. Yang, Q. Gu, Z. Liu, T. Xie, Q. Jin, P. Zheng, S. Xu and W. Zhu, *Bioorg. Chem.*, 2020, **95**, 103525.
- 12 N. Lolak, S. Akocak, S. Bua, R. Sanku and C. Supuran, *Bioorg. Med. Chem.*, 2019, **27**, 1588–1594.
- 13 E. Havránková, J. Csöllei, D. Vullo, V. Garaj, P. Pazdera and C. Supuran, *Bioorg. Chem.*, 2018, **77**, 25–37.
- 14 B. Żołnowska, J. Sławiński, K. Szafranski, A. Angeli, C. Supuran, A. Kawiak, M. Wieczór, J. Zielińska, T. Bączek and S. Bartoszewska, *Eur. J. Med. Chem.*, 2018, **143**, 1931–1941.
- 15 K. Bergant, M. Janežič, K. Valjavec, I. Sosič, S. Pajk, M. Štampar, B. Žegura, S. Gobec, M. Filipič and A. Perdih, *Eur. J. Med. Chem.*, 2019, **175**, 330–348.
- 16 X. Zhou, K. Lin, X. Ma, W. K. Chui and W. Zhou, *Eur. J. Med. Chem.*, 2017, **125**, 1279–1288.
- 17 S. Narva, S. Chitti, S. Amaroju, D. Bhattacharjee, B. Rao, N. Jain, M. Alvala and K. Sekhar, *Bioorganic Med. Chem. Lett.*, 2017, **27**, 3794–3801.
- 18 B. Sever, M. Altıntop, M. Radwan, A. Özdemir, M. Otsuka, M. Fujita and H. Ciftci, *Eur. J. Med. Chem.*, 2019, **182**, 111648.
- 19 Z. Brzozowski, F. Sa and M. Gdaniec, *Eur. J. Med. Chem.*, 2000, **35**, 1053–1064.
- 20 L. Moreno, J. Quiroga, R. Abonia, J. Ramírez-Prada and B. Insuasty, *Molecules*, 2018, **23**, 1956.
- 21 H. Dmytro, Z. Borys, V. Olexandr, G. Andrzej and L. Roman, *J. Med. Chem.*, 2020, **55**, 8630–8641.
- 22 G. Bagnolini, D. Milano, M. Manerba, F. Schipani, J. Ortega, D. Gioia, F. Falchi, A. Balboni, F. Farabegoli, F. De Franco, J. Robertson, R. Pellicciari, I. Pallavicini, S. Peri, S. Minucci, S. Girotto, G. Di Stefano, M. Roberti and A. Cavalli, *J. Med. Chem.*, 2020, **63**, 2588–2619.
- 23 S. Farooq and Z. Ngaini, *Tetrahedron Lett.*, 2020, **61**, 151416.
- 24 S. Mirzaei, F. Hadizadeh, F. Eivand, F. Mosaffa and R. Ghodsi, *J. Mol. Struct.*, 2020, **1202**, 127310.
- 25 S. Burmaoglu, S. Ozcan, S. Balcioglu, M. Gencel, S. Noma, S. Essiz, B. Ates and O. Algul, *Bioorg. Chem.*, 2019, **91**, 103149.
- 26 G. Wang, W. Liu, Z. Gong, Y. Huang, Y. Li and Z. Peng, *Bioorg. Chem.*, 2020, **95**, 103565.
- 27 L. Rahman, D. Voeller, R. Monzur, L. Stan, C. Allegra, C. Barrett, F. Kaye and M. Zajac-Kaye, *Cancer Cell*, 2004, **5**, 341–351.
- 28 L. Taddia, D. D'Arca, S. Ferrari, C. Marraccini, L. Severi, G. Ponterini, Y. Assaraf, G. Marverti and M. Costi, *Drug Resist. Updat.*, 2015, **23**, 20–54.
- 29 R. Xing, H. Zhang, J. Yuan, K. Zhang, L. Li, H. Guo, L. Zhao, C. Zhang, S. Li, T. Gao, Y. Liu and L. Wang, *Eur. J. Med. Chem.*, 2017, **139**, 531–541.
- 30 A. Lauria, M. Ippolito and A. M. Almerico, *Comput. Biol. Chem.*, 2009, **33**, 386–390.
- 31 A. Lauria, I. Abbate, C. Patella, A. Martorana, G. Dattolo and A. M. Almerico, *Eur. J. Med. Chem.*, 2013, **62**, 416–424.
- 32 A. Lauria, M. Ippolito and A. M. Almerico, *J. Mol. Graph. Model.*, 2009, **27**, 712–722.
- 33 A. Lauria, M. Ippolito and A. M. Almerico, *QSAR Comb. Sci.*, 2009, **28**, 387–395.
- 34 A. Lauria, S. Mannino, C. Gentile, G. Mannino, A. Martorana and D. Peri, *Bioinformatics*, 2020, **36**, 1562–1569.
- 35 D. Chen, A. Jansson, D. Sim, A. Larsson and P. Nordlund, *J. Biol. Chem.*, 2017, **292**, 13449–13458.
- 36 H. Berman, J. Westbrook, Z. Feng, G. Gilliland, T. Bhat, H. Weissig, I. Shindyalov and P. Bourne, *Nucleic Acids Res.*, 2000, **28**, 235–242.
- 37 P. Kathiriya, V. Patel and D. Purohit, *J. Chem. Pharm. Res.*, 2013, **5**, 103–107.
- 38 NCI-60 Screening Methodology, https://dtp.cancer.gov/discovery_development/nci-60/methodology.htm, accessed April 17, 2020.
- 39 Schrödinger Release 2017–2, *LigPrep*, Schrödinger, LLC, New York, 2017.
- 40 Schrödinger Release 2017-2: *Protein Preparation Wizard*, Epik, Schrödinger, LLC, New York, 2017.
- 41 J. Banks, H. Beard, Y. Cao, A. Cho, W. Damm, R. Farid, A. Felts, T. Halgren, D. Mainz, J. Maple, R. Murphy, D. Philipp, M. Repasky, L. Zhang, B. Berne, R. Friesner, E. Gallicchio and R. Levy, *J. Comput. Chem.*, 2005, **26**, 1752–1780.
- 42 G. M. Sastry, M. Adzhigirey and W. Sherman, *J. Comput. Aided. Mol. Des.*, 2013, **27**, 221–234.
- 43 R. Friesner, R. Murphy, M. Repasky, L. Frye, J. Greenwood, T. Halgren, P. Sanschagrin and D. Mainz, *J. Med. Chem.*, 2006, **49**, 6177–6196.
- 44 T. Halgren, R. Murphy, R. Friesner, H. Beard, L. Frye, W. Pollard and J. Banks, *J. Med. Chem.*, 2004, **2**, 1750–1759.
- 45 R. Friesner, J. Banks, R. Murphy, T. Halgren, J. Klicic, D. Mainz, M. Repasky, E. Knoll, M. Shelley, J. Perry, D. Shaw, P. Francis and P. Shenkin, *J. Med. Chem.*, 2004, **47**, 1739–1749.
- 46 W. Sherman, T. Day, M. Jacobson, R. Friesner and R. Farid, *J. Med. Chem.*, 2006, **49**, 534–553.
- 47 W. Sherman, H. Beard and R. Farid, *Chem. Biol. Drug Des.*, 2006, **67**, 83–84.
- 48 Maestro, Version 9.3, Schrödinger, LLC. New York 2012.
- 49 H. Zhong, L. Tran and J. Stang, *J. Mol. Graph. Model.*, 2009, **28**, 336–346.
- 50 H. Luo, J. Wang, W. Deng and K. Zou, *Med. Chem. Res.*, 2013, **22**, 4970–4979.
- 51 H. Wang, R. Aslanian and V. Madison, *J. Mol. Graph. Model.*, 2008, **27**, 512–521.
- 52 M. Jacobson, R. Friesner, Z. Xiang and B. Honig, *J. Mol. Biol.*, 2002, **320**, 597–608.

